Low-intensity transcranial focused ultrasound changes pain-associated behaviors by modulating pain processing brain circuits

Min Gon Kim[1,†], Kai Yu[1,†], Raghda Fouda[2], Donovan Argueta[2], Stacy Kiven[2], Yunruo Ni[1], Xiaodan Niu[1], Qiyang Chen[3], Kang Kim[3,4], Kalpna Gupta[2], and Bin He[1,5*]

[1]Department of Biomedical Engineering, Carnegie Mellon University, Pittsburgh, PA 15213

[2]Department of Medicine, University of California at Irvine, Irvine, CA 92697

[3]Department of Medicine, University of Pittsburgh, Pittsburgh, PA 15261

[4]Department of Bioengineering, University of Pittsburgh, Pittsburgh, PA 15261

[5]Neuroscience Institute, Carnegie Mellon University, Pittsburgh, PA 15213

†These authors contributed equally to this work.

*Corresponding Author: Bin He, Ph.D., bhe1@andrew.cmu.edu

ABSTRACT

Despite enormous efforts made in clinical pain research, there is still a need to identify a novel non-pharmacological solution due to critical side-effects. Low-intensity transcranial focused ultrasound (tFUS) is an emerging non-invasive neuromodulation technology with high spatial specificity and deep brain penetration. Here, we demonstrate that tFUS stimulation at pain processing brain circuits significantly affects behavioral responses to noxious stimuli in *in vivo* mouse models. We developed a tightly-focused 128-element random array ultrasound transducer with a dynamic focus steering for targeting small mice brains, and found that a single-session tFUS to the primary somatosensory cortex (S1) attenuates heat pain sensitivity in wild-type mice, bidirectionally modulate thermal and mechanical hyperalgesia in humanized mouse model of sickle cell disease as a function of ultrasound pulse repetition frequency (PRF), and targeting deeper cortical structure (e.g., insula) led to a sustained behavioral change associated with heat hyperalgesia. Furthermore, we found that multi-session tFUS to S1 and insula resulted in a long-lasting suppression of heat pain-associated behaviors in older sickle mice and confirmed the safety of the tFUS protocol. These profound experimental evidence of tFUS-induced non-invasive modulation of pain-related behaviors from short- to long-term effects may facilitate the next-generation chronic pain treatment.

Key words: pain, neuromodulation, focused ultrasound, sickle cell disease

Introduction

Multidimensional impact of the chronic pain has been closely linked to various aspects of the quality of life and a greater risk of developing physical and mental health problems[1,2,3]. The quest for treating chronic pain with non-pharmacologic treatment remains a priority as numerous reports have raised concern about the increased risks of opioids with drug abuse, overdose, and addiction[4,5,6]. To completely or significantly reduce the need of pharmacologic options for chronic pain treatment, a range of neuromodulation methods have been developed, in particular targeting brain circuits involved in pain pathways, from implanted devices such as deep brain stimulation (DBS) to non-invasive techniques including transcranial direct current stimulation (tDCS) and transcranial magnetic stimulation (TMS)[7,8,9,10,11]. DBS is well recognized as an effective treatment technique for movement disorders and a potential treatment option for chronic pain, providing reversible alteration of brain function with the use of electrodes surgically placed in the targeted area of the deep brain[7,8]. Despite substantial improvements of quality of life in patients, the clinical use of this method is limited by the invasive surgical intervention[7,9,10,11]. This critical limitation has led to the development of alternative approaches for non-invasive neuromodulation, such as tDCS and TMS, which has shown to be effective for non-invasive brain disorder treatments such as depression[12] and chronic pain[13,14]. However, tDCS and TMS are limited as both affect a broad area rather than a specific targeted brain region and have difficulty to stimulate deep brain structures[9,10].

Low-intensity transcranial focused ultrasound (tFUS) is a promising neuromodulation technology capable of non-invasive modulation of neuronal activity in

specific brain regions with a high degree of specificity and penetration depth compared with other brain stimulation techniques[15,16,17]. Prior studies have provided experimental evidence that tFUS non-invasively elicits or inhibits brain activity by varying tFUS parameters[15,16,17,18,19] and treats a myriad of neurological disorders including Parkinson's disease[20,21], Alzheimer's disease[22,23], and depression[24]. Inspired by these promising results, researchers have extended the use of tFUS to demonstrating a feasibility of pain management by stimulating the right anterior thalamus using pulsed tFUS at 650 kHz to increase thermal pain thresholds in healthy individuals[25], posterior frontal cortex using continuous tFUS at 8 MHz to induce mood improvement in chronic pain patients[26], and periaqueductal gray (PAG) using pulsed tFUS at 650 kHz to attenuate formalin-mediated nociceptive activity on the spinal cord dorsal horn in chemical-induced pain model in rats[27].

In spite of promising studies achieved, a number of fundamental questions remain unresolved. First, numerous studies have shown that multiple brain areas are activated by noxious stimuli such as S1 and the secondary somatosensory cortex (S2), insula, thalamus, anterior cingulate cortex, basal ganglia, and PAG[28,29,30], yet how tFUS can achieve improved behavioral pain responses by interacting with the pain perception and processing brain circuits remains unknown. Second, none of the prior studies have provided the effect of directing tFUS to a control region near the targeted brain location[25,26,27], which is yet to be established. Thus, an unmet need is to determine whether the achieved analgesic effect is specific to tFUS stimulation to the certain brain region. Third, human-based pain research has provided critical evidence of understanding and treating pain, but effective and safe pain management remains elusive due to the limited capability of evaluating and assigning pain a simple numerical value

through self-report of pain[31] as well as interventional experiments with various pain assays in humans[31,32]. Currently, well-established rodent models of chronic pain have shown similarity to human genetic and pathological disease and a potential for translational pain research[33,34,35,36]. In particular, pain in sickle cell disease can be chronic as well as unpredictable, widespread, and recurrent episodes of acute pain. Therefore, there is an urgent need to consider critical aspects, as described above, for establishing an effective and safe pain treatment approach via tFUS stimulation using the humanized mouse model of sickle cell disease.

Here, we present tFUS-induced modulation of pain-associated behaviors, from short-term to long-lasting modulatory effects, by stimulating specific brain regions involved in pain processing in wild-type mice and humanized mouse model of sickle cell disease (HbSS-BERK) exhibiting constitutive chronic hyperalgesia similar to that observed in persons with sickle cell disease[34,37,38,39]. The hypothesis is that specific brain circuits involved in pain perception and processing can be modulated by tFUS stimulation, thus resulting in a change (i.e., deterioration or amelioration) of pain-associated behaviors elicited by various types of noxious stimulus in the well-established rodent models of acute and chronic pain. By using a 128-element highly-focused random array transducer, we demonstrated the performance of high spatial specificity along with a dynamic focus steering capability to adapt the small sized mouse brain, which could not be achieved by using single-element ultrasound transducers that have been widely used in the ultrasound neuromodulation field. In addition, we investigated short-term and sustained effect of the single-session tFUS stimulation to the various pain processing brain regions including S1, insula, and thalamus on the pain-associated behaviors evoked by noxious heat, cold, and

mechanical stimuli in wild-type and HbSS-BERK mice. Furthermore, we assessed a long-lasting suppression of heat pain-associated behaviors via the multi-session tFUS stimulation at the selected pain processing brain circuits such as S1 and insula in aged HbSS-BERK mice. Lastly, to determine whether the achieved modulatory effect is specific to tFUS stimulation within safe exposure limits without adverse effects, we further implemented a comprehensive set of control experiments, behavior and histological evaluations.

Results

Experimental configuration and characterization of the 128-element random array transducer with targeting validation

Fig. 1a schematically demonstrates the proposed experimental setup comprised of various types of behavioral tests, tFUS stimulation with multiple control groups, and video assessment with data analysis. We recorded and examined behavioral nocifensive responses to heat, cold, and mechanical stimuli before and after tFUS stimulation to three different brain regions along with control groups with and without the light anesthesia during treatment period. In the behavioral experiments, various controls including negative control group (i.e., no tFUS stimulation, but maintaining the same experimental procedures) and sham-treated group (i.e., applying tFUS to a control brain structure near the bregma) were added to rule out potential confounding factors of anesthesia, auditory side-effects, and other global effects from the observed tFUS-mediated modulation of pain-associated behaviors (Fig. 1b). A customized 128-element random array ultrasound

transducer (H276) working at a center frequency of 1.5 MHz was used to electronically steer the direction of the focused ultrasound beam with controllable parameters including tone-burst duration (TBD) of 200 μs, pulse repetition frequency (PRF) of 40 Hz and 3 kHz, ultrasound duration (UD) of 400 ms, inter-sonication interval (ISoI) of 4 s, and total sonication time of 10 min, 20 min, and 1 h as depicted in Fig. 1c.

To enable a three dimensional (3D) high spatial specificity when directing the tFUS onto small brain targets in mice, we customized and developed a spherically-concave, highly-focused 128-element random array ultrasound transducer (i.e., H276) working at a fundamental frequency of 1.5 MHz (See details in Methods). To transmit focused ultrasound (FUS) pulses through the skull in the experiment, the customized FUS probe for mice models (Fig. 2a and Supplementary Fig. 1a, the random element spatial configuration is illustrated in the inset) was driven by a Vantage 128 research ultrasound platform. In free water, the measured coherent axial and lateral focal sizes (-3 dB contour) were 1.36 mm and 0.46 mm, respectively (Fig. 2b-c). Further, when electronically steering the ultrasound focus in free water, the depicted submillimeter focal size (Fig. 2d) enabled for the precise spatial targeting at specific mouse brain circuits without mechanically moving the transducer. Fig. 2e demonstrates the side-lobe suppression when the ultrasound energy was coherently focused and laterally steered (Supplementary Fig. 1b-c shows the respective line profiles of ultrasound pressures normalized to corresponding scan's maximum output). In the presence of a freshly excised mouse skull (without skull base) immersed in degassed water, the transcranial ultrasound focus was still spatially tight with a lateral specificity of 0.84 mm and an axial specificity of 1.71 mm (-3 dB contour) (Fig. 2f). The acoustic insertion loss due to the skull was measured as approximately 10.3

dB. To better understand the ultrasound field distribution within a complete mouse skull cavity, we built a computer simulation model mimicking the same acoustic aperture of H276 (Supplementary Fig. 1d). The simulated coherent focal size (Supplementary Fig. 1e) in free water was commensurate with that of H276 in physical measurement (Fig. 2c). In the simulation, the inclusion of mouse skull base generated certain standing wave pattern (see supplementary materials for quantifications of standing waves in computer simulations), while the focal size was measured as 2.30 mm in axial direction and 0.82 mm in lateral direction (Fig. 2g and Supplementary Fig. 1f-g with co-registrations of a mouse brain atlas in coronal and sagittal planes).

To validate the accuracy of ultrasound beam steering and the spatial location of transcranial ultrasound focus in the *in vivo* experiments, the setup of the intracranial electrophysiological recordings was integrated with the tFUS experimental setup to examine whether time-locked neuronal activations could be observed during tFUS stimulation. The administered ultrasound peak-peak pressure behind the female mouse skull was measured as 90.4 kPa when the ultrasound focus was steered and targeted into the hindlimb of the S1 (S1HL) in the left hemisphere of the brain in 2 mice subjects, at which the intracranial electrode was placed. The tFUS stimulation with tone-burst duration of 200 μs, ultrasound duration of 100 ms, and PRF of 3 kHz elicited the instantaneous neuronal activities, which was illustrated in the peri-stimulus time histogram (PSTH, Fig. 2h) and the raster plot (Fig. 2i). In contrast, when the ultrasound focus was steered and applied to a sham location at the midline (ΔX = -1.77 mm, ΔY = 1.225 mm, relative to the recording site at the S1HL), the evoked neuronal spiking activity was not observed (Supplementary Fig. 1h-i). In addition, the negative observations were

found when the ultrasound focus was moved by ±1.5 mm in X- and Y-axis from the recording site at the S1HL (Supplementary Fig. 1j-m). These evaluations support the precise tFUS targeting when steering and directing ultrasound focus onto the specific brain circuits for modulating the pain.

Short-term attenuation of heat pain-related behaviors in male and female wild-type mice

Assessment of pain-related behaviors from a nociceptive stimulus has been widely used to quantify and evaluate nociception in non-communicating subjects such as rodents[32,39,40,41,42,43]. However, it is unclear whether stimulus-evoked behavioral responses could be altered by tFUS stimulation to brain regions intimately involved in processing sensory aspect of the pain such as S1. Therefore, we tested whether certain tFUS stimulation parameters at the specific brain structure could yield a significant change in thermal pain-associated behaviors compared to pre-stimulation baseline and sham-treated behavioral change. For this purpose, we chose and applied a single-session of tFUS stimulation with a low PRF as this parameter has been shown to induce higher spike rates of inhibitory neurons in S1[44]. In addition, unilateral effect of tFUS stimulation to the left S1HL on the behavioral nocifensive reactions to the noxious heat stimulus with pre-determined temperature of 53°C was blindly assessed through comparing the latency of the withdrawal response of the ipsilateral (left) hind paw with the contralateral (right) hind paw[45] (Fig. 3a). Driving ultrasound pulses with a PRF of 40 Hz to stimulate left S1HL resulted in a notable increase in latency time to react to the pain caused by the noxious heat, represented as averaged Δ hind paw withdrawal latency

(hPWL = contralateral (right) hPWL - ipsilateral (left) hPWL), compared to pre-stimulation baseline in male wild-type mice (Fig. 3b, left panel, ***p=0.0009, animal number N=8 for 3 min after tFUS; *p=0.0248, N=8 for 8 min after tFUS; one-way ANOVA with Friedman test; Fig. 3b, right panel, absolute change of Δ hPWL over baseline of 6.85 ± 1.68 s for 3 min after tFUS and 3.06 ± 0.67 s for 8 min after tFUS). However, the averaged Δ hPWL treated by sham ultrasound did not lead to a prominent change compared to its baseline value (Fig. 3c, left panel, p>0.05, N=8 for 3 min and 8 min after sham treatment; one-way ANOVA with Friedman test). In addition, when comparing the effect of tFUS stimulation with a sham control at the same measurement time, a remarkable increase of Δ hPWL was observed (Fig. 3c, left panel, $^{\#\#}p$=0.0016, N=8 for 3 min after tFUS and sham treatment; $^{\#}p$=0.0135, N=8 for 8 min after tFUS and sham treatment; t-test with Mann-Whitney test; Fig. 3c, right panel, absolute change of Δ hPWL over sham treatment of -0.05 ± 0.34 s for pre-stimulation baseline, 6.70 ± 1.42 s for 3 min after tFUS, and 2.55 ± 1.00 s for 8 min after tFUS).

Next, we examined the gender related differences in terms of tFUS-induced modulation of pain-related behaviors. Concerning the effect of gender, it has been demonstrated that the majority of patients with chronic pain are females who display more sensitivity to pain than the males do, which may result in different effect of pain modulation[39,46,47,48]. We found a remarkable increase in latency differences between the ipsilateral (left) and contralateral (right) hind paw withdrawal in female wild-type mice through the single-session tFUS at left S1HL against the baseline (Fig. 3d, left panel, **p=0.0016, N=8 for 3 min after tFUS; *p=0.0119, N=8 for 8 min after tFUS; one-way ANOVA with Friedman test), but the treatment effect (i.e., attenuated heat pain-related

behavior) was relatively smaller than that observed in male wild-type mice (Fig. 3e, right panel, absolute change of Δ hPWL over baseline of 4.19 ± 1.04 s for 3 min after tFUS and 3.72 ± 0.65 s for 8 min after tFUS). In addition, we observed a significant increase in Δ hPWL between the effect of tFUS stimulation and sham treatment, whereas sham treatment had little effect on Δ hPWL compared to the baseline value (Fig. 3e, left panel, $^{\#}p$=0.018, N=8 for 3 min after tFUS and sham treatment; $^{\#}p$=0.0159, N=8 for 8 min after tFUS and sham treatment; t-test with Mann-Whitney test; p>0.05, N=8 for 3 min and 8 min after sham stimulation; one-way ANOVA with Friedman test; Fig. 3e, right panel, absolute change of Δ hPWL over sham treatment of 0.09 ± 0.49 s for pre-stimulation baseline, 3.10 ± 1.24 s for 3 min after tFUS, and 3.16 ± 0.56 s for 8 min after tFUS). Based on the results, the single-session tFUS stimulation with PRF of 40 Hz to S1HL, but not sham location, led to a significant suppression of heat pain-related behaviors in both male and female wild-type mice with gender difference in stimulation effect.

Short-term modulation of thermal (heat and cold) and mechanical hyperalgesia in female HbSS-BERK mice

We next explored the effect of tFUS stimulation with a well-established female mouse model of acute and chronic pain. Previous work has shown that humanized sickle cell mice (HbSS-BERK) constitutively exhibit significant thermal and mechanical hyperalgesia compared to genetic control mice (HbAA-BERK), which is similar to that observed in SCD patients[35,36,37,38]. Using this mouse model, three brain locations (S1, thalamus, and insula) were chosen as key brain structures for pain processing and perception and stimulated[28,29,30]. These features, as described above, prompt the

question of whether stimulating such brain regions could affect pain processing and perception, which could consequently have impact on thermal and mechanical hyperalgesic behaviors in HbSS-BERK mice. To test this, a single-session of tFUS stimulation with a low or a high PRF was administered to the S1HL, thalamus, and insula in female HbSS-BERK mice and behavioral responses to noxious heat, cold, and mechanical stimuli were investigated before and after tFUS stimulation with multiple controls (Fig. 4a).

We first examined the response to heat stimuli measured as paw withdrawal latency (PWL) difference between the ipsilateral (left) and contralateral (right) hind paws (Δ hPWL) with the single-session tFUS with a PRF of 40 Hz or 3 kHz in female HbSS-BERK sickle mice. Application of ultrasound pulses with PRF of 40 Hz to target left S1HL resulted in a significant suppression of heat pain-related behaviors, which was represented as a marked change in the averaged Δ hPWL of 4.40 ± 1.29 s and 4.17 ± 1.26 s for 3 min and 8 min after tFUS, respectively as compared to the baseline value of -0.50 ± 0.37 s (Fig. 4b, left panel, $^{**}p$=0.0051, N=10 for 3 min and 8 min after tFUS; one-way ANOVA with Friedman test; Fig. 4b, right panel, absolute change of Δ hPWL over baseline of 4.90 ± 1.34 s for 3 min after tFUS and 4.67 ± 1.29 s for 8 min after tFUS) as well as negative control and sham treatment at 3 and 8 min after treatment (Fig. 4c, left panel, $^{\#}p$=0.0272, N=10 for 3 min after tFUS with the PRF of 40 Hz and negative control; $^{\#}p$=0.0481, N=10 for 3 min after tFUS with the PRF of 40 Hz and sham treatment; $^{\#}p$=0.0327, N=10 for 8 min after tFUS with the PRF of 40 Hz and negative control; $^{\#\#}p$=0.0035, N=10 for 8 min after tFUS with the PRF of 40 Hz and sham treatment; one-way ANOVA with Kruskal-Wallis test; Fig. 4c, middle panel, absolute change of Δ hPWL

over sham treatment of -0.59 ± 0.39 s for pre-stimulation baseline, 4.48 ± 1.33 s for 3 min after tFUS with the PRF of 40 Hz, and 4.74 ± 1.17 s for 8 min after tFUS with the PRF of 40 Hz; Fig. 4c, right panel, absolute change of Δ hPWL over negative control of -0.34 ± 0.31 s for pre-stimulation baseline, 4.88 ± 1.11 s for 3 min after tFUS with the PRF of 40 Hz, and 4.19 ± 1.28 s for 8 min after tFUS with the PRF of 40 Hz). However, the change in Δ hPWL induced by sham treatment as well as in the negative control was not apparent compared to the pre-treatment baseline (Fig. 4c, left panel, $p>0.05$, N=10 for negative control and sham treatment; one-way ANOVA with Friedman test). Moreover, we found a negative value of Δ hPWL modulated by the single-session tFUS stimulation with the PRF of 3 kHz to the left S1HL, which indicates a decreased contralateral (right) hind paw latency compared to latency of ipsilateral (left) hind paw. Regarding these distinct behavioral responses to tFUS stimulation paradigms, bidirectional modulation of sensitivity to heat was prominently observed in terms of PRF values from 40 Hz to 3 kHz (Fig. 4c, left panel, $^{###}p=0.0003$, N=10 for 3 min after tFUS with PRF of 40 Hz and 3 kHz; $^{####}p<0.0001$, N=10 for 8 min after tFUS with PRF of 40 Hz and 3 kHz; one-way ANOVA with Kruskal-Wallis test). These results demonstrate that tFUS stimulation with a low (40 Hz) or a high (3 kHz) PRF at S1HL is linked to attenuation or exacerbation of heat hyperalgesia in female HbSS-BERK mice.

Next, we addressed the question whether a single-session of tFUS stimulation could modulate cold hyperalgesia in HbSS-BERK mice by comparing the paw withdrawal frequency (PWF) of each ipsilateral (left) and contralateral (right) hind paw (Δ hPWF = contralateral (right) hPWF - ipsilateral (left) hPWF) during a testing period of 2 min. As compared to pre-application baseline, the single-session tFUS stimulation with the PRF

of 40 Hz to left S1HL or insula led to a significant decrease in the cold hyperalgesia represented as a negative value of Δ hPWF (Supplementary Fig. 2a, left panel, $^{*}p$=0.0371, N=10 for 8 min after tFUS with the PRF of 40 Hz at S1HL; Supplementary Fig. 2a, middle panel, $^{**}p$=0.0020, N=10 for 8 min after tFUS with the PRF of 40 Hz at insula; t-test with Wilcoxon matched-pairs signed rank test). In addition, the effect of the single-session tFUS stimulation at left S1HL, insula, and thalamus on the Δ hPWF differed significantly from sham group at 8 min after sham treatment (Fig. 4d, $^{\#}p$=0.0460, N=10 for 8 min after tFUS with the PRF of 40 Hz at S1HL and sham treatment; $^{\#}p$=0.0355, N=10 for 8 min after tFUS with the PRF of 40 Hz at insula and sham treatment; $^{\#}p$=0.0225, N=10 for 8 min after tFUS with the PRF of 40 Hz at thalamus and sham treatment; t-test with Mann-Whitney test). However, neither tFUS at thalamus nor control groups such as negative control and sham treatment resulted in a remarkable difference of the frequency of contralateral (right) and ipsilateral (left) hind paw withdrawals compared to the baseline (Supplementary Fig. 2a, right panel, ns, p>0.05, N=10 for 8 min after tFUS with the PRF of 40 Hz or 3 kHz at thalamus; t-test with Wilcoxon matched-pairs signed rank test; Fig. 4d, p>0.05, N=10 for 8 min after negative control and sham treatment; t-test with Wilcoxon matched-pairs signed rank test). As summarized, the single-session tFUS with the PRF of 40 Hz at S1HL or insula, but not thalamus region, is effective for ameliorating cold hyperalgesia in HbSS-BERK mice.

We further studied the effect of a single-session tFUS stimulation on mechanical hyperalgesia in HbSS-BERK mice by comparing the threshold of the withdrawal response of the ipsilateral (left) hind paw with the contralateral (right) hind paw in response to the application of a series of von Frey monofilaments. When left S1HL or insula was

stimulated with tFUS at a PRF of 40 Hz, a significant reduction in mechanical hyperalgesia calculated as Δ hind paw withdrawal threshold (Δ hPWT = contralateral (right) hPWT - ipsilateral (left) hPWT) was observed compared to the baseline value (Supplementary Fig. 2b, left panel, $^{*}p$=0.0313, N=10 for 8 min after tFUS at S1HL; Supplementary Fig. 2b, middle panel $^{*}p$=0.0156, N=10 for 8 min after tFUS at insula; t-test with Wilcoxon matched-pairs signed rank test) as well as sham-treated or negative control mice (Fig. 4e, $^{\#\#}p$=0.0011, N=10 for 8 min after tFUS at S1HL and negative control; $^{\#\#}p$=0.0025, N=10 for 8 min after tFUS at insula and negative control; $^{\#}p$=0.0232, N=10 for 8 min after tFUS at S1HL and sham treatment; $^{\#}p$=0.0482, N=10 for 8 min after tFUS at insula and sham treatment; one-way ANOVA with Kruskal-Wallis test). In addition, tFUS with the PRF of 3 kHz at left S1HL exacerbated mechanical hypersensitivity as represented a lower threshold of the withdrawal response of the contralateral (right) hind paw compared to the ipsilateral (left) hind paw, which is similar to that observed in behavioral responses to heat stimuli (Fig. 4e, $^{\#\#\#}p$=0.0009, N=10 for 8 min after tFUS with the PRF of 3 kHz or 40 Hz at S1HL; $^{\#\#}p$=0.0022, N=10 for 8 min after tFUS with the PRF of 3 kHz at S1HL and tFUS with the PRF of 40 Hz at insula; one-way ANOVA with Kruskal-Wallis test). Based on the experimental results, the single-session tFUS stimulation with the PRF of 40 Hz at S1HL or insula can significantly reduce, but the tFUS with the PRF of 3 kHz to S1HL significantly exacerbate mechanical hyperalgesia in female HbSS-BERK mice.

Sustained and long-lasting modulatory effect of heat hyperalgesia in female HbSS-BERK mice

Given that the single-session tFUS stimulation led to a significant, but short-term change (i.e., at least 8 min) in the attenuation of thermal and mechanical hyperalgesia, we next investigated whether sustained tFUS effect on heat hyperalgesia could be obtained by targeting deeper brain structures such as insula and thalamus. The mice modulated with the single-session tFUS at the PRF of 40 Hz in the left insula showed much longer latency of the contralateral (right) hind paw in comparison to the latency of ipsilateral (left) hind paw for 30 min when comparing with pre-stimulation baseline (Fig. 5b, left panel, $^{**}p$=0.0094, N=10 for 8 min after tFUS; $^{*}p$=0.0288, N=10 for 30 min after tFUS; one-way ANOVA with Friedman test; Fig. 5b, right panel, absolute change of Δ hPWL over baseline of 3.54 ± 1.49 s for 3 min after tFUS with the PRF of 40 Hz, 5.43 ± 1.15 s for 8 min after tFUS with the PRF of 40 Hz, 4.58 ± 1.55 s for 30 min after tFUS with the PRF of 40 Hz, and 2.77 ± 0.73 s for 60 min after tFUS with the PRF of 40 Hz). This effect was specific to the single-session tFUS stimulation with the PRF of 40 Hz as neither control groups including negative control and sham treatment nor tFUS with the PRF of 3 kHz significantly differed from their respective baseline values (Fig. 5c, left panel, p>0.05, N=10 for negative control, sham stimulation, and tFUS with the PRF of 3 kHz; one-way ANOVA with Friedman test). Significant differences were also observed between tFUS with the PRF of 40 Hz and controls such as negative control and sham treatment (Fig. 5c, left panel, $^{\#}p$=0.0203, N=10 for 3 min after tFUS with the PRF of 40 Hz and negative control; $^{\#}p$=0.0311, N=10 for 3 min after tFUS with the PRF of 40 Hz and sham treatment; $^{\#\#}p$=0.0035, N=10 for 8 min after tFUS with the PRF of 40 Hz and negative control; $^{\#\#\#}p$=0.0003, N=10 for 8 min after tFUS with the PRF of 40 Hz and sham treatment; $^{\#}p$=0.0197, N=10 for 30 min after tFUS with the PRF of 40 Hz and negative control;

$^{\#\#}p$=0.0025, N=10 for 30 min after tFUS with the PRF of 40 Hz and sham treatment; $^{\#\#}p$=0.0084, N=10 for 60 min after tFUS with the PRF of 40 Hz and negative control; one-way ANOVA with Kruskal-Wallis test; Fig. 5c, middle panel, absolute change of Δ hPWL over sham treatment of 1.05 ± 0.63 s for pre-stimulation baseline, 4.77 ± 1.44 s for 3 min after tFUS with the PRF of 40 Hz, 7.15 ± 1.62 s for 8 min after tFUS with the PRF of 40 Hz, 6.77 ± 1.61 s for 30 min after tFUS with the PRF of 40 Hz, and 2.61 ± 1.44 s for 60 min after tFUS with the PRF of 40 Hz; Fig. 5c, right panel, absolute change of Δ hPWL over negative control of 1.31 ± 0.72 s for pre-stimulation baseline, 5.17 ± 1.47 s for 3 min after tFUS with the PRF of 40 Hz, 6.60 ± 1.58 s for 8 min after tFUS with the PRF of 40 Hz, 5.55 ± 1.56 s for 30 min after tFUS with the PRF of 40 Hz, and 4.56 ± 1.13 s for 60 min after tFUS with the PRF of 40 Hz). In contrast, delivering tFUS with PRF of 40 Hz in the thalamus resulted in a less pronounced behavioral responses compared to targeting the insula. Indeed, stimulating thalamus led to some changes in Δ hPWL with a tendency towards attenuating heat pain-related behavior, but this tendency was not statistically significant compared to the baseline (Fig. 5d, left panel, p>0.05, N=10 for 3, 8, 30, and 60 min after tFUS with PRF of 40 Hz; one-way ANOVA with Friedman test) or controls (Fig. 5d, right panel, p>0.05, N=10 for negative control and sham treatment; one-way ANOVA with Kruskal-Wallis test), except two measurements (Fig. 5d, right panel, $^{\#}p$=0.0104, N=10 for 8 min after tFUS with the PRF of 40 Hz and sham treatment; $^{\#}p$=0.0277, N=10 for 60 min after tFUS with the PRF of 40 Hz and negative control; one-way ANOVA with Kruskal-Wallis test). Thus, we did not find statistically significant evidence of robust and sustained modulatory effect by targeting the thalamus region with the same tFUS paradigms and experimental setup targeted to the insula. Taken together,

these observations reveal that single-session tFUS stimulation with PRF of 40 Hz to insula, but not thalamus location, is effective for a sustained attenuation (i.e., 30 min) of hyperalgesia to heat stimuli in female HbSS-BERK mice.

We further explored whether a long-lasting attenuation of pain behaviors for more than 1 h could be achieved in older and female sickle mice, as treatment for chronic pain in older adults poses a major challenge to treat. Prior studies have demonstrated that older and female patients experience prolonged hospital stays with drug treatments for chronic pain, and aged and female sickle mice show a significant increase in hyperalgesia for painful stimuli compared to younger and male sickle mice[35,36,37,38]. We observed a significant change in behavioral response to heat stimulus represented as the averaged hPWL in female HbSS-BERK mice ranging from 11 to 15 month-old compared to the value in female HbSS-BERK mice ranging from 5 to 9 month-old (Supplementary Fig. 3a, $^{\#}p$=0.0481, N=26 for female HbSS-BERK mice from 5 to 9 months old and N=15 for female HbSS-BERK mice from 11 to 15 months old; t-test with Mann-Whitney test), which demonstrates significantly higher heat hyperalgesia in older female HbSS-BERK mice. Next, we investigated the effect of multi-session tFUS stimulation to the selected brain regions including S1HL and insula or sham treatment for 14 days with 1 h per day on the behavioral responses to noxious heat stimulus in older female HbSS-BERK mice (Fig. 6a). The multi-session tFUS with the PRF of 40 Hz to the left S1HL and insula for 14 days resulted in a significantly longer latency of the contralateral (right) hind paw withdrawal than the value of ipsilateral (left) hind paw withdrawal when compared with pre-stimulation baseline (Fig. 6b, left panel, $^{*}p$=0.0156, N=6 for tFUS to S1HL; $^{*}p$=0.0469, N=6 for tFUS to insula; t-test with Wilcoxon one-tailed signed rank test) as well as behavioral change

in the sham-treated group (Fig. 6b, right panel, $^{\#}p$=0.019, N=4 for sham treatment and N=6 for tFUS to S1HL; $^{\#}p$=0.0436, N=4 for sham treatment and N=6 for tFUS to insula; t-test with one-tailed Mann-Whitney test). Given the time interval of 2 h between tFUS stimulation and behavioral measurement, the effect of multi-session tFUS to S1HL and insula lasted up to 2 h after 14 days of 1 h stimulation, but not after sham treatment. Together, these results suggest that multi-session tFUS stimulation with the PRF of 40 Hz at S1HL or insula can induce a long-lasting (i.e., 2 h) amelioration of heat hyperalgesia in older female HbSS mice which exhibit significantly increased constitutive thermal hyperalgesia compared with younger and male mice.

PRF: key component for modulation of pain-related behaviors

In some prior studies, tFUS stimulation with the PRF of 10 Hz[25] or 1.5 kHz[49] could change thermal or mechanical pain thresholds, respectively and lower duty cycle has been shown to induce inhibitory effect in cortical and thalamic neuronal activity[50,51]. Thus, we further investigated whether tFUS with specific PRF values within a low duty cycle, but maintaining same transmitted ultrasound energy, could lead to a reduction of sensitivity to a nociceptive stimulus in a similar manner as tFUS with the PRF of 40 Hz, as described above. In this control experiment, additional stimulation paradigms, in particular a combination of PRF and tone-burst duration (TBD) were selected to match the same duty cycle of 0.8% (Fig. 7a, additional parameter 1 (AP1) with PRF of 10 Hz and TBD of 800 μs; additional parameter 2 (AP2) with PRF of 3 kHz and TBD of 2.67 μs) and applied at S1HL without changing the rest of the experimental setup. Neither tFUS stimulation with AP1 nor AP2 resulted in a significant change in heat pain-related behavior

in HbSS-BERK mice compared to pre-stimulation (Fig. 7b, $p>0.05$, N=7 for 3 and 8 min after tFUS with AP1 and AP2 at S1HL; one-way ANOVA with Friedman test). Therefore, the specific PRF is a key to the modulation in behavioral responses to noxious stimuli in HbSS-BERK mice.

tFUS Safety evaluation

Next, with a view towards safety evaluation, we first tested whether tFUS stimulation would negatively impact normal motor activities and functions. We investigated neuromuscular coordination through rotarod testing after single- and multi-session tFUS to superficial and deep brain regions (Fig. 8a, left panel). The rotarod test has been well-established to evaluate motor coordination and balance by assessing the time of falling from a programmed rotating rod[52,53]. After the single-session tFUS with a PRF of 40 Hz at S1HL or thalamus and multi-session tFUS stimulation with the PRF of 40 Hz at S1HL or insula for 14 days, we did not find any significant difference in the averaged latency to fall compared with pre-stimulation baseline (Fig. 8a, middle panel, $p>0.05$, N=11 for 60 min after single-session tFUS at S1HL and thalamus; t-test with Wilcoxon matched-pairs signed rank test; Fig. 8b, left panel, $p>0.05$, N=4 for 60 min after multi-session tFUS at S1HL; $p>0.05$, N=6 for 60 min after multi-session tFUS at insula; one-way ANOVA with Friedman test) and the value from negative control (Fig. 8a, right panel, $p>0.05$, N=11 for 60 min after negative control and single-session tFUS at S1HL and thalamus; one-way ANOVA with Kruskal-Wallis test) or sham treatment (Fig. 8b, right panel, $p>0.05$, N=4 for 60 min after multi-session sham treatment; one-way ANOVA with Kruskal-Wallis test). Similarly, the average time spent on the rotarod from the negative

control or the multi-session sham treatment was not markedly different from the baseline values (Fig. 8a, middle panel, $p>0.05$, N=11; t-test with Wilcoxon matched-pairs signed rank test; Fig. 8b, left panel, $p>0.05$, N=4; one-way ANOVA with Friedman test), which indicates that single- and multi-session tFUS stimulation at cortical and deep brain structures does not induce remarkable adverse effect on normal motor functions in HbSS-BERK mice.

To further explore the effect of tFUS stimulation on the structural integrity of tissues and nuclear morphology within treated brain region, we performed a double blind analysis of the histological features of the brain using hematoxylin and eosin (H&E) and Prussian blue-stained sections, and determined apoptosis using terminal deoxynucleotidyl transferase dUTP nick end labeling (TUNEL) assay after chronic treatment for 1 h daily over 14 days with tFUS to the left S1HL, insula, or thalamus with control groups including negative control, sham treatment, and high dose tFUS in HbSS-BERK sickle and naïve HbAA-BERK control mice. We first evaluated structural tissue integrity in terms of hemorrhage, hemosiderin-laden macrophages, and inflammatory and apoptotic cells in H&E slides of brain tissue by comparing ipsilateral (treated) brain regions with the contralateral (untreated) brain locations as internal controls in 10 randomly selected fields[54]. We did not observe any significant difference in structural integrity of the tissues in the ipsilateral brain location treated by the multi-session tFUS stimulation with PRF of 40 Hz and those in the contralateral brain region in HbSS-BERK and HbAA-BERK mice (Fig. 8c and Supplementary Fig. 6c-d, respectively) as well as those from the multi-session sham treatment (Fig. 8c), multi-session negative control (Supplementary Fig. 6a-b), and even multi-session high-dose tFUS treatment (i.e., 8 times of the currently used

peak-peak pressure) (Supplementary Fig. 6e-f). In addition, neurons exhibited normal morphology with their characteristic basophilic (blue) cytoplasm, large nuclei, and prominent nucleoli, and many neurons have small round nuclei satellite cells which are oligodendroglia cells in gray matter. Next, we quantified iron accumulation in brain tissues along with the multi-session tFUS stimulation with control groups as cell-free heme in the tissues due to hemolysis is a critical feature of sickle cell pathobiology with adverse effects on pain[55]. Neither tFUS with PRF of 40 Hz nor control groups such as negative control and high-dose tFUS stimulation exhibited a presence of ferric (iron) deposits in both ipsilateral and contralateral brain regions (Supplementary Fig. 6a-f). Furthermore, immunohistochemical analysis using TUNEL assay confirmed that no significant difference was observed in the number of apoptotic cells per approximately 1,000 total number of cells treated with the multi-session tFUS stimulation with the PRF of 40 Hz at left S1HL, insula, or thalamus when compared to the contralateral (untreated) brain region as internal controls in HbSS-BERK and HbAA-BERK mice (Fig. 8c and Supplementary Fig. 6c-d). In addition, multi-session control groups including negative control, sham treatment, and high-dose tFUS stimulation resulted in similar number of apoptotic cells between ipsilateral and contralateral brain locations (Fig. 8c and Supplementary Fig. 6a-b and e-f). These results suggest that the multi-session tFUS stimulation in this study throughout the chronic use did not lead to any adverse effect on organ damage or sickle cell pathobiology. Thus, prolonged tFUS treatment appears to be functionally and structurally safe in HbSS-BERK sickle and HbAA-BERK control mice.

Discussion

We have conducted well-controlled preclinical studies to quantitatively assess the effect of tFUS neuromodulation to non-invasively exacerbate or ameliorate pain-associated behaviors by targeting pain processing brain circuits in wild-type mice and well-established humanized mouse model of sickle cell pain. We report that a single- and multi-session tFUS stimulation distinctly and non-invasively interacted with brain circuits involved in pain perception and processing, leading to a significant modulation of pain-related behaviors, which is effective in both short- and long-term, in the wild-type and humanized HbSS-BERK sickle mice.

Previous studies have demonstrated that optogenetic activation of parvalbumin (PV) neurons, one of the GABAergic neurons, at 40 Hz in the hippocampus or S1 triggers activation of immune cells[56,57] or positively impacts mechanical nociception[58], respectively. In contrast, vibroacoustic treatment at 40 Hz leads to a beneficial effect on a chronic pain disorder such as Fibromyalgia with widespread musculoskeletal pain[59.60]. As the biological mechanism of 40 Hz stimulation on the nervous and immune systems is still unknown, the present study provides an understanding of how repeated ultrasound pulses at 40 Hz to the multiple brain regions modulate chronic pain-associated behaviors. We provide experimental evidence of amelioration of heat pain sensitivity in wild-type mice and modulation of thermal (heat and cold) and mechanical hyperalgesia in humanized sickle cell mice by stimulating several pain processing brain circuits. Application of the single-session of tFUS with a PRF of 40 Hz at left S1HL or insula resulted in a significant change in the withdrawal latency (heat), frequency (cold), and threshold (mechanical) of the contralateral (right) hind paw compared to the ipsilateral

(left) hind paw, from short-term to sustained stimulatory effect. In addition, a longer-lasting attenuation of heat hyperalgesia was achieved by multi-session tFUS with the PRF of 40 Hz to left S1HL or insula in aged HbSS-BERK mice. However, tFUS with the same stimulation parameter (i.e., PRF of 40 Hz) at thalamus did not show a statistically significant amelioration of heat and mechanical pain behaviors. Another notable finding is that single-session tFUS with higher PRF (i.e., 3 kHz) at S1HL, but not insula and thalamus, promotes heat and mechanical pain-associated behaviors in HbSS-BERK mice. Consistent with prior studies demonstrating critical contribution of CaMKIIα on chronic pain exaggeration in HbSS-BERK mice[34,61] and tFUS-mediated distinct action potential waveforms and significant spike rates of S1 in transgenic CaMKIIα mice and PV mice[44], promoted heat and mechanical pain-associated behaviors were observed when the S1HL was targeted by the tFUS. Other than the significant reduction of pain-related behaviors, this finding could also have clinical significance for potentially treating people with insensitivity to physical pain by tFUS with PRF of 3 kHz to S1 region. Successful application of the tFUS with the PRF of 40 Hz and 3 kHz to S1HL, insula, and thalamus, demonstrates the ability to target additional pain processing brain circuits including anterior cingulate cortex and amygdala in the future studies, for elucidating the effect of tFUS stimulation on pain via these regions.

We conducted a comprehensive set of control experiments to validate that the achieved analgesic effect is specific to tFUS stimulation by minimizing the effects of confounding factors. First, when it comes to applying tFUS to the brain *in vivo*, we placed the mouse onto the stereotactic frame in order to securely hold its head by using anesthesia. Although light anesthesia was used in this study and the effect of tFUS on

pain-related behaviors was compared with controls including negative control and sham groups, analgesic effect of isoflurane remains an important factor. To examine the possibility of the effect of anesthesia on the observed pain-related behaviors, specialized experimental setup (i.e., head-restrained awake naturally walking mouse in the air-lifted platform) was used to directly measure tFUS modulatory effect without using anesthesia (Supplementary Fig. 3a). The wild-type mice treated by single-session tFUS with the PRF of 40 Hz at left S1HL showed a significant increase in latency difference of the contralateral (right) hind paw withdrawal compared to the value from ipsilateral (left) hind paw withdrawal when compared to pre-stimulation baseline (Supplementary Fig. 3b, left panel, $^{*}p$=0.0187, N=6 for 3 and 8 min after tFUS; one-way ANOVA with Friedman test; Supplementary Fig. 3b, right panel, absolute change of Δ hPWL over baseline of 2.19 ± 0.69 s for 3 min after tFUS and 2.01 ± 0.51 s for 8 min after tFUS) and the response from sham-stimulated mice (Supplementary Fig. 3c, left panel, $^{\#\#}p$=0.0043, N=6 for 3 min after tFUS; $^{\#\#}p$=0.0065, N=6 for 8 min after tFUS; t-test with Mann-Whitney test; absolute change of Δ hPWL over sham treatment of 0 ± 0.17 s for pre-stimulation baseline, 2.52 ± 0.75 s for 3 min after tFUS, and 1.93 ± 0.68 s for 8 min after tFUS). However, sham-treated mice showed no significant change in Δ hPWL compared to the baseline value (Supplementary Fig. 3c, left panel, p>0.05, N=6 for 3 and 8 min after sham-treatment; one-way ANOVA with Friedman test). These findings are complemented by the observations on HbSS-BERK sickle mice that remained responsive to mechanical and thermal stimuli while recording the nociceptor activity in the second order neurons electrophysiologically under isofluorane anesthesia[62]. Taken together, tFUS modulatory effect was also significant in head-fixed awake mice, which was similar to those observed

in the above results; thus light anesthesia used in this study is deemed to have relatively negligible effect on tFUS-induced modulation of pain-associated behavioral response, although the post-surgical pain in the head-fixed awake mice may inevitably introduce a confounding pain source for hyperalgesia assessments.

Second, prior studies have reported that altered nocifensive behaviors were frequently observed in the repeated hot-plate test, which is caused by non-nociceptive factors such as learning or habituation[63,64,65,66]. As an additional control experiment, we examined the inter-experimental day intervals to rule out the potential contribution of non-nociceptive factors to the observed tFUS-mediated analgesic effect on the pain-related behaviors (Supplementary Fig. 4a). After measurement of baseline latency from noxious heat stimuli (hPWL) at every 3-4 days, we found a significant decrease in the hPWL from the measurement on day 10-11 compared to the measured hPWL on day 1 in HbSS-BERK mice (Supplementary Fig. 4b, $*p=0.0133$, N=12; one-way ANOVA with Friedman test). In contrast, the effect of inter-experimental time interval of 6-7 days was not apparent when compared to hPWL in Day 1 (Supplementary Fig. 4b, $p>0.05$, N=12; one-way ANOVA with Friedman test). This control experiment suggests that inter-experimental time interval of 6-7 days did not significantly present a tendency for learned or habituated behaviors, which has minimized impact on the tFUS-induced modulation of pain-related behaviors.

In addition to the increased need for spatial specificity, the small size of the mouse skull cavity poses technical challenges for the tFUS application due to the presence of standing waves. The standing wave pattern in a medium has been shown as occurrence of oscillating patterns of peak and valleys in the wave amplitude. This oscillating pattern

that resembles a zebra-striped shape in the wave-amplitude map is mostly used for implying the presence of standing waves in the medium. To better evaluate this physical phenomenon and to quantify the extent of standing waves formed intracranially by the ultrasound pressure waves in computer simulations, two standing wave quantification metrics, i.e., standing wave ratio (SWR) and R-factor (see Methods section for more details), were employed to characterize the standing wave existing in the small mouse skull cavity, especially when steering tFUS focus onto certain cortical and subcortical targets for managing pain. We numerically calculated both SWR and R-factors for all tFUS scenarios acquired from computer simulations (see Methods section for more details on computer simulations). Unsurprisingly, the coherent ultrasound focus within the mouse skull cavity as shown in Fig. 2g has larger SWR and R-factor values than the coherent ultrasound focus (Supplementary Fig. 1e) in the free water does (Supplementary Fig. 5c-d). No significant difference was found in the SWR comparisons between the tFUS pressure fields when the focus was steered onto the Sham location or onto the S1HL target (Supplementary Figs. 5a and 5e), as well as between the pressure fields when the focus was steered onto the thalamus or onto the insula (Supplementary Figs. 5a and 5g). Similarly, the overall R-factor when the tFUS focus was steered onto the thalamus was not significantly different from the value when it was steered onto the insula (Supplementary Fig. 5b), but the slice-wise comparisons illustrate significantly less R-factor (Supplementary Fig. 5h) and SWR (Supplementary Fig. 5g) values in certain slice range (i.e., slice 20-30) when the ultrasound focus was targeted at the thalamus. Overall, the increased standing wave patterns due to the presence of the full mouse skull cavity as well as due to the ultrasound beam steering merit further investigations and efforts for

minimization in order to fully harness the enhanced spatial targeting capability of the 128-element random ultrasound array transducer.

To prevent tFUS-induced thermal effect and tissue damage for the translation of the new scientific findings in preclinical studies, low-intensity (I_{SPTA}: 461.10 mW/cm^2 measured through female mouse skull) was used to adhere to regulation for safe use of diagnostic ultrasound ($I_{SPPA} \leq 190$ W/cm^2) stipulated by the Food and Drug Administration (FDA)[67,68]. Given the low-intensity range (< 3 W/cm^2), normal motor coordination and balance using the rotarod test was observed in single- and multi-session tFUS-treated mice compared to motor performance from pre-stimulated mice. Furthermore, the safety of tFUS stimulation was evaluated through histological assessment such as H&E and immunohistochemistry (IHC) from small to large animal models including mouse[69,70], rat[71,72], rabbit[73], sheep[74], nonhuman primate (NHP)[75,76] as histology is a critical endpoint for the non-clinical evaluation of medical devices and biomaterials. Here, we rigorously investigated the interactions between mice brain tissues and multi-session tFUS stimulation for 14 days with 1 h per day in humanized HbSS-BERK and naïve control mice (HbAA-BERK). Three different histological assessments using H&E, iron, and TUNEL stains showed that tFUS stimulation had no negative impact on the tissue structural integrity and nuclear morphology within tFUS treated brain region. The effect of sickle cell phenotype was not evident in the histopathology of the brain regions of interest in our study such as S1HL and insula. However, the pyknotic neuronal cells and iron deposition encountered in brain sections outside of our regions of interest were consistent with the previously described neuropathologic abnormalities in sickle cell phenotype mice, as increased apoptotic Purkinje cells[77,78] and the presence of pyknotic neurons in the

hippocampus and cerebellum[79]. Furthermore, a reliable safety window of tFUS stimulation was established with the use of the high-dose tFUS stimulation, which enables for prevention of short- and long-term adverse stimulation effects for clinical implications.

The findings in this study are promising, but several questions and limitations should be considered. First, although we provide evidence-based behavioral analysis by investigating multiple aspects such as various targeted brain regions with several controls and various types of nociceptive stimuli, a better understanding of how tFUS interacts with cellular and physiological function of pain processing brain circuits is needed. The mechanism of action behind this study is likely to be complicated as several critical factors could be independently or simultaneously involved in chronic pain amelioration or exacerbation. For example, a growing body of pain research reported that activation of brain microglial due to peripheral nerve injury led to chronic pain[80], and glutamate which is a major excitatory neurotransmitter played a crucial role in transmission of a nociceptive impulse in both acute and chronic pain[81]; serotonin was one of the key contributors to chronic pain[58], and GABAergic interneurons had essential inhibitory role in regulating pain-related signals[82]; low Dopamine levels were linked to the painful symptoms[83]. In HbSS-BERK sickle mice modulation of serotonin and dopamine in the rostral ventromedial medulla and PAG regions of the brain, respectively through diet and companionship led to significant amelioration of mechanical and thermal hyperalgesia[84]. These sickle mice also show significant glial activation in the spinal cords[55,85]. It is likely that tFUS may be modulating the serotonergic and dopaminergic inhibitory pain pathway and inhibiting glial activation in sickle mice which needs to be investigated. Thus, building upon the observed findings along with the established tFUS stimulation paradigms,

investigation and elucidation of molecular and electrophysiological features could have important implications for gaining a better insight on how tFUS directly affects neuronal activity in pain processing brain circuits and pain-related behaviors. Second, previous studies reported that very thin mouse skull had little effect on the propagation of ultrasound energy, up to a center frequency of 5 MHz[86,87,88]. Despite relatively well-preserved spatial distributions of the ultrasound focus through thin mouse skull, it is important to establish more accurate tFUS targeting approach due to the inter-mouse skull shape variability along with significant improvements in spatial resolution of H276. In this study, targeted brain structures were estimated and registered by Allen Mouse Brain Atlas[89,90,91], a widely used 3D map of the whole mouse brain, but this high-resolution anatomic reference may not be representative of the entire mice populations, especially the humanized sickle cell mice used in this study. Thus, the establishment of each mouse's skull shape acquired by computed tomography could enable us not only to characterize and address inter-mouse skull shape variations but also to improve ultrasound focusing by applying phase aberration correction technique with 128-element random array ultrasound transducer.

In summary, we demonstrate, for the first time to the best of our knowledge, that non-invasive low-intensity tFUS stimulation to cortical and deep brain regions involved in pain perception and processing resulted in a significant modulation in thermal and mechanical pain-associated behaviors from short-term (i.e., at least 8 min) to long-term (i.e., up to 2 h) modulatory effects in wild-type mice and well-established humanized mouse model of sickle cell pain. Our observations evince critical experimental evidence for the efficacy and safety of the tFUS neuromodulation with state-of-the-art multi-element

highly focused random array transducer for clinical pain management. The highly promising preclinical results suggest that tFUS has a translational potential to become an effective, non-addictive, non-pharmacological, non-invasive device-based neuromodulation technique for managing chronic pain without causing adverse effects.

Materials and Methods

Animals

Wild-type mice: Male and female wild-type mice (C57BL/6J) were purchased from the Jackson Laboratory. A pair of mice was used for breeding and housed at constant temperature on a 12-h light/dark cycle at Carnegie Mellon University. Adult mice (14 male and 16 female mice) ranging from 3 to 6 month-old were used to reduce age-dependent changes in nocifensive behaviors. All studies used in wild-type mice were approved by the Institutional Animal Care and Use Committee (IACUC) of Carnegie Mellon University.

Transgenic mice: The transgenic BERK mice are on a mixed genetic background (FVB/N, 129, DBA/2, C57BL/6, and Black Swiss) with murine α and β globin knockouts ($\alpha^{-/-}$ and $\beta^{-/-}$) with sickle mice expressing >99% human sickle hemoglobin S (HbS), demonstrating many severe features of SCD including chronic pain; and control mice expressing normal human HbA[92,93]. Mice were generated in-house by cross-breeding homozygous (SS) males with hemizygous (AS) females[92]. Mice were bred and raised with ad libitum access to food and water on a 12-h light/dark cycle in conventional housing. Age-matched HbSS-BERK mice ranging from 5 to 9 month-old, and 11 to 15 month-old

were used to match age-related behaviour changes. All studies in HbSS-BERK and HbAA-BERK were approved by the IACUC of Carnegie Mellon University and the Long Beach VA medical Centre, Long Beach, and complied with National Institutes of Health guidelines.

General procedures: Mice were anesthetized using 3% isoflurane at 1L/min oxygen flow for induction and 1-1.25% isoflurane with 0.2 L/min oxygen flow at 100% for maintenance. For tFUS targeting evaluation via electrophysiological recordings, mice were anaesthetized using 3% isoflurane at 1L/min oxygen flow for induction and 1.5-2% isoflurane at 0.5L/min oxygen flow at 100% during recordings. The eyes of mice subjects were protected with ophthalmic ointment. Heating pad was used to maintain body temperature in anesthetized mice and the rectal temperatures were frequently monitored during the experiments.

Head-restrained awake naturally walking mice: The head fixation platform (Mobile HomeCage, Neurotar Ltd, Helsinki, Finland) was used to rule out the possibility of the anesthesia effect on the observed pain-related behaviors in wild-type mice. Surgery for a head plate's application to the mouse's skull was conducted about a week before behavioral experiments. The wild-type mice were placed in the stereotaxic frame under isoflurane (2.5-3%). The skin surface on the head was sterilized by quickly wiping with swabs soaked in 70% EtOH and betadine three times. The entire surface of parietal, interparietal, and frontal bones was exposed by carefully removing a flap of skin using scissors and forceps. The exposed skull region was degreased with a cotton swab soaked in acetone. A small amount of dental cement (Stoelting Co, Wood Dale, IL, USA) and a few drops of tissue adhesive (3M Vetbond, 3M, Saint Paul, MN, USA) were mixed and

stirred to generate a viscous liquid. A thin layer of this mixture was applied onto the surface of exposed bones. After approximately 5 min, a small amount of cyanoacrylate glue (Loctite 401, Henkel, Henkel Düsseldorf, Germany) was applied onto the bone-contacting surface of the metal head plate and then the metal head plate against the interparietal and frontal bones was slightly pressed. The dental cement powder mixed with cyanoacrylate glue was applied into the small round holes on the frontal and dorsal parts of the head plate.

The multi-element random array ultrasound transducer and its performance

The H276 is a spherically-concave, 128-element random ultrasound array transducer, which was customized and manufactured by Sonic Concepts, Inc. (Bothell, WA, USA). The radius of the acoustic aperture was 8.5 mm, and it had a 15 mm diameter of acoustic exit plane. Each sub-aperture diameter was 0.8 mm, and all elements were arranged in a random distribution with a 1 mm pitch. The -3 dB operating frequency band was approximately 1.35-1.60 MHz, and centered at 1.50 MHz. This FUS probe was driven by a Vantage 128 research ultrasound platform (Verasonics, Kirkland, WA, USA) through a DL-260 connector, and an external power supply (QPX600DP, Aim-TTi, Cambridgeshire, UK) was connected to the Vantage system to avoid any significant voltage droop during each ultrasound burst (i.e., the tone burst duration of 200 μs). During the in vivo experiment, the acoustic aperture of H276 was filled up with ultrasound transmission gel (Aquasonic Ultrasound gel, Parker Laboratories, Inc., Fairfield, NJ, USA) to couple the focused ultrasound to the mouse head.

Ex-vivo transcranial ultrasound pressure scanning: To characterize the tFUS pressure and intensity fields in the presence of mice skull (only the skull top), a customized *ex-vivo* 3D pressure mapping system with a needle hydrophone (HNR500, Onda Corporation, Sunnyvale, CA, USA) was employed. A 3-axial positioning stage (XSlide, Velmex, Inc., Bloomfield, NY, USA) was used to drive the spatial scanning of the hydrophone submerged in degassed water. A mouse skull sample was freshly procured from euthanized mice subjects, and it was placed between the H276 probe (acoustic aperture submerged in water) and the hydrophone to reproduce the tFUS experimental setup.

In-silico transcranial ultrasound pressure simulations within a whole mouse skull cavity: The tFUS spatial profiles were further studied in computer simulations (Sim4Life, Zurich Med Tech ag., Zurich, Switzerland) with a whole mouse skull cavity. The full-wave acoustic solver based upon a non-uniform finite difference time domain method could provide rapid and accurate estimations of ultrasound field residing within a realistic mouse skull model. The micro-CT images were acquired from Rangos Research Center Animal Imaging Core Facility in University of Pittsburgh. In the simulations, all the entities were assumed to be submerged in water (mass density: 1000 kg/m^3, speed of sound: 1500 m/s), and the cortical bone's physical properties were assigned with mass density 2,200 kg/m^3, speed of sound 3,300 m/s [44], and attenuation coefficient 81.8 Np/m (based on the tissue properties database of The Foundation for Research on Information Technologies in Society).

Standing wave characterizations: We employed two metrics to quantify the presence of standing wave within the region covering the spatial peak pressure of the

coherent or steered transcranial focused ultrasound. The R-factor metric measures the deviation from the mean pressure by comparing the amplitude of the peak p_{max} to the valley p_{min} over a region with an average p_{avg} as observed in Eq. 1[94].

$$\text{R-factor} = \frac{p_{\max} - p_{\min}}{p_{\text{avg}}} \tag{1}$$

Furthermore, we used the second metric, standing wave ratio (SWR) for quantifying the intracranial standing waves which calculates the pressure ratio between the wave antinode ($p_{antinode}$) and wave node (p_{node}) and thus quantifies the extent of the wave being pure or partial standing wave[95]. This metric is calculated over a region of pressure waves as in Eq. 2 and is commonly reported in the unit of decibels.

$$\text{SWR} = \frac{p_{\text{antinode}}}{p_{\text{node}}} \tag{2}$$

For both metrics, a higher value confers an indication that there is an increased presence of standing waves in the region of interest.

Experimental configuration in tFUS stimulation

tFUS stimulation procedures: The Vantage 128 ultrasound driving system was used to excite the 128-element random array transducer with controllable parameters and electronically steer the ultrasound focus. As shown in Fig. 1b, tFUS stimulation was applied with a center frequency of 1.5 MHz, TBD of 200 μs, UD of 400 ms, ISoI of 4 s, total sonication time of 10 min, 20 min, and 1 h, and PRF of 40 Hz and 3 kHz. For the ultrasound parameter study (Fig. 7), duty cycle was maintained as 0.8%, but different combinations of PRF and TBD were selected (i.e., AP1: PRF of 10 Hz with TBD of 800

μs and AP2: PRF of 3 kHz with TBD of 2.67 μs) and applied without modifying other tFUS experimental setups.

tFUS targeting procedures: To estimate targeted brain structures and co-register with the H276, Allen Mouse Brain Atlas was used to determine coordinate information of ultrasound focus by visually aligning both X-axis of the transducer's surface with the posterior end of zygomatic structure and Y-axis of transducer with the mouse's rostral-caudal line. The ultrasound focus was then electronically steered and applied to the targeted brain region as noted in Table 1 (validated with computer simulations). A thin layer of ultrasound transmission gel was applied to couple the ultrasound beam to the scalp after mouse hair was moisturized with deionized water.

Validation of tFUS targeting using electrophysiological recordings: Mouse head was stabilized in a stereotaxic frame under the isoflurane (see Methods section for more details on animals). A local piece of scalp was removed using surgical scissors to make the skull exposed. The pre-identified brain locations were found based on the skull suture lines and the Allen Mouse Brain Atlas[89,90,91]. The exposure of the brain with a cranial window (1-2 mm in diameter) was performed by using a stereotaxic high-speed drill (Model 1474, David Kopf Instruments, Tujunga, CA, USA) with stereomicroscope (V-series otology microscope, JEDMED, St. Louis, MO, USA). After 32-channel single shank electrode array (A1x32-Poly3-10mm-50-177, NeuroNexus, Ann Arbor, MI, USA) was inserted at the region of interest with a stereotaxic manipulator arm (David Kopf Instruments, Tujunga, CA, USA), the intracranial electrophysiological recordings were conducted through the micro-electrode array connected to a TDT Neurophysiology Workstation (Tucker-Davis Technologies, Alachua, FL, USA). The multi-unit activities

were sorted using OpenSorter (Tucker-Davis Technologies, Alachua, FL, USA) and then analyzed using Offline Analysis Tool (Tucker-Davis Technologies, Alachua, FL, USA) in MATLAB v9.10.0 (The MathWorks, Inc., Natick, MA, USA).

Experimental configuration in pain-related behavior assessment and evaluation

All behavioral experiments were conducted during the light cycle of the animals. As a habituation step, all the wild-type and HbSS-BERK mice were acclimatized to the environment for 30 min and then each behavioral test apparatus for 30 min (hot-plate test and cold-plate test) and 10 min (von Frey test and rotarod test) at constant temperature, which was repeated for at least 2 days before performing the actual behavioral testing. To prevent potential confounding factors such as learning or habituation, same set of mice was minimally repeated in behavioral experiments at inter-experimental time interval of 6-7 days.

Heat hyperalgesia: After habituation step, temperature of hot-plate (Ugo Basile, Collegeville, PA, USA) was calibrated to set time of the elicited withdrawal response within 8-15 s. If there was no nociceptive response within 30 s, the mouse was immediately removed from the hot-plate chamber to prevent any potential heat-related tissue injury. Based on the temperature calibration, temperature of hot-plate was determined as 53 °C for wild-type mice and 52 °C for HbSS-BERK mice, respectively. Mice were gently placed onto the surface of the hot-plate and the latency of withdrawal response to heat stimuli applied to hind paws was determined by time to first sign of nociception such as hind paw licking or flicking or jumping from the hot-plate, represented as a hPWL. A lower hPWL indicates greater heat hyperalgesia and detailed behavioral

analysis was followed. The pre-stimulation baseline was averaged and obtained after measurement was repeated for 2-3 times with an inter-measurement interval of 5 min. After treatment with tFUS and controls (i.e., sham stimulation or negative control), behavioral response to heat was measured at 3, 8, 30, and 60 min after single-session treatment or 2 h after multi-session treatment. All behavioral experiments on hot-plate test were videotaped for further validation and blind experiment design.

Cold hyperalgesia: The temperature of cold-plate (Ugo Basile, Collegeville, PA, USA) was set at 4 °C based on the prior study[39,92]. Mice were gently placed onto the surface of the cold-plate and hPWF over a 2 min period was determined. Higher hPWF indicates greater cold hyperalgesia and detailed behavioral analysis was followed. To prevent a potential cold-related risk of injury or death, cold hypersensitivity measurements were conducted no more than 2 sessions on a single experiment day. After treatment with tFUS and controls (i.e., sham stimulation or negative control), behavioral response to cold was measured at 8 min after treatment. All behavioral experiments on cold-plate test were videotaped for further validation and blinded experimental design.

Mechanical hyperalgesia: Mice were gently placed into glass container on the wire mesh table. Minimum threshold of von Frey filaments (Stoelting Co, Wood Dale, IL, USA) that could elicit withdrawal response was determined by the up-down method[96,97]. Briefly, a series of von Frey filaments, ranging from 0.04 g to 8.0 g, were applied to the plantar surface of each hind paw with a force enough to bend the filament for 1-2 s and an inter-stimulus interval of at least 5 s. Ascending or descending mechanical stimuli were applied in a consecutive fashion starting with the 1.0 g monofilament. In the absence of the paw withdrawal response to a filament, a stronger stimulus was applied, whereas in the

presence of the paw withdrawal response to a filament, the next weaker stimulus was applied. When reaching 5th filament, positive adjustment factor (+ 0.5×final filament value) was added to the final filament value, if there was no response to the 5th filament of the sequence. However, if there was a withdrawal response to the 5th filament, negative adjustment factor (- 0.5×final filament value) was added to the final filament value.

Motor performance: Motor coordination and balance were assessed by an accelerating rotarod apparatus[98] (Ugo Basile, Collegeville, PA, USA). Mice were gently placed onto the rotating rod which was programmed to have a gradient increase of revolutions per minute (rpm) from 3 rpm to 72 rpm over 5 min testing period. The mouse was immediately placed back on the rod after falling up to 3 times and the integral of time spent on the rod (i.e., latency to fall) was measured. After treatment with tFUS and controls (i.e., sham stimulation or negative control), behavioral response to rotating rod was measured at 60 min after treatment.

Behavioral analysis: Given the performance of H276 capable of specifically targeting left hemisphere of the brain region, the unilateral effect of tFUS on nocifensive behaviors was investigated based on the modified hot-plate test method[45] and calculated as follows: Δ hPWL (s) = contralateral (right) hPWL- ipsilateral (left) hPWL, which addressed the limitation of classical hot-plate test. In addition to the hot-plate test, behavioral responses to the cold and mechanical stimuli were assessed and calculated, respectively as follows: Δ hPWF = contralateral (right) hPWF- ipsilateral (left) hPWF and Δ hPWT = contralateral (right) hPWT- ipsilateral (left) hPWT.

Histology

To rigorously evaluate tFUS safety, histological assessments were conducted with a chronical treatment for 14 days with 1 h per day as a critical endpoint. For this study, both HbSS-BERK and their genetic control, HbAA-BERK, mice were used as it has been demonstrated that HbSS-BERK mice have constitutive cellular damage and apoptosis in the brain[77,78]. We compared the contralateral (untreated) brain locations as internal controls with ipsilateral (treated) brain regions in HbAA-BERK control mice also to rigorously examine the safety of the applied tFUS treatment by ruling out intrinsic lesions in the HbSS-BERK mice brains. Whole brain sections were examined for neuropathologic changes, but histopathological findings and images are reported only from the tFUS-treated and analogous untreated contralateral region. In addition, we set and used four different groups including multi-session 1) tFUS stimulation, 2) high-dose tFUS stimulation (i.e., 8 times of the currently used peak-peak pressure), 3) negative control, and 4) sham treatment. After 14 day treatments, mice were humanely euthanized and the brains were collected immediately following euthanasia and fixed in 10% neutral buffered formalin (HT501128, Sigma-Aldrich, St. Louis, MO, USA) based on the established mouse brain fixation protocol[84] then embedded in paraffin blocks for sectioning. After deparaffinization and rehydration with ethanol gradient, 4 μm thickness sections were stained with H&E, iron stain kit (AR15811-2, Agilent, Santa Clara, CA, USA), and TUNEL assay kit (ab206386, Abcam, Cambridge, UK) per manufacturer's guidelines. Double blind histological investigations on the coronal tissue sections for ipilateral and contralateral hemispheres were conducted by a pathologist with expertise in clinical pathology and sickle mice histology. H&E stained sections were analyzed for the presence or absence of hemorrhage, and signs of tissue damage (i.e., necrosis,

intracellular red blood cell breakdown (hemosiderin-laden macrophages), inflammation, and macrophage infiltration. The percentage of sections in which histologic findings were detected were assessed for both left and right hemispheres in 10 randomly selected fields, 4 sections per specimen[54]. In addition, sections stained for iron were analyzed for the presence or absence of ferric (iron) deposits as a sign of damage in the brain regions. Furthremore, sections stained with TUNEL assay and methyl green counterstain were analyzed with Nikon Eclipse TE300 light microscope with 2x zoom on 4x and 20x objectives for the presence or absence of apoptotic cells in the brain regions.

Statistics

Data are expressed as mean ± standard error of the mean (s.e.m.) unless specified and analyzed using Prism software (GraphPad Prism, GraphPad Software, San Diego, CA, USA). Repeated measures and non-parametric one-way ANOVA with Friedman test and paired and non-parametric t-test with Wilcoxon matched-pairs signed rank test were used to compare withdrawal responses relative to the pre-stimulation baseline. In these tests, ns: not significant and p-value of $<0.05^{*}$, $<0.01^{**}$, and $<0.001^{***}$ was assumed to be statistical significance. No matching and non-parametric one-way ANOVA with Kruskal-Wallis test and unpaired and non-parametric t-test with Mann-Whitney test were used to compare withdrawal responses relative to values from other parameters in the same measurement time. In these tests, p-value of $<0.05^{\#}$, $<0.01^{\#\#}$, $<0.001^{\#\#\#}$, and $<0.0001^{\#\#\#\#}$ was considered statistically significant.

Author Contributions

B.H., K.Y. initiated the concept; B.H., K.Y., M.G.K., K.G. designed the studies; M.G.K. conducted neuromodulation, behavior experiments, and analyzed behavior data; K.Y., Y.N., D.A. performed behavior data assessments; K.G., D.A., S.A. produced sickle cell mice; K.Y., K.K., Q.C. developed the multi-element array transducer; K.Y., M.G.K., X.N. characterized the transducer array and validated the ultrasound targeting; R.F., D.A. performed histology assessments; M.G.K., K.Y. co-wrote the original draft; B.H., K.G., R.F., D.A., K.K., Q.Y., Y.N. contributed to reviewing and editing of the manuscript. B.H. and K.G. supervised the work.

Acknowledgements

This work was supported in part by NIH EB029354, NS124564, MH114233, AT009263, NS096761, EB021027, and HL147562. S.K. was supported by Diversity Supplement 3R01HL147562-03S, and D.A. was supported by a University of California President's Fellowship and Giannini Foundation Fellowship. *The content is solely the responsibility of the authors and does not necessarily represent the official views of the National Institutes of Health*.

The authors would like to thank Shahriar Noroozizadeh on a part of the programming for standing wave quantifications and Dr. Yijen Wu from Rangos Research Center Animal Imaging Core for providing micro-CT images of mice; and Natalie Garcia and Reina Lomelli, University of California Irvine with availability of transgenic mice. We also want

to thank Kyle Morrison from Sonic Concepts, Inc. for providing consultation in customizing the H276 probe.

Cartoons in Figures 1a–b, 2f, 3a(left), 4a(bottom), 5a(left), 6a, 8a(left), Supplementary Figures 3a–b, and 4a(left) were created with BioRender.com.

Competing Interest Statement

B.H., K.Y. and X.N. are co-inventors of pending patent applications on tFUS technique. The remaining authors declare that the research was conducted in the absence of any commercial or financial relationships that could be construed as a potential conflict of interest.

Disclosures: KG: Honoraria: *Novartis* and *CSL Behring*. Research Grants: *Cyclerion*, *1910 Genetics, Novartis*, *Grifols*, *Zilker*, *UCI Foundation and SCIRE Foundation*

Data Availability Statement

The data supporting the conclusions of this study are provided in the paper and supplementary information. Additional behavioral and electrophysiological data will be made available at public repository when the paper is accepted. Source data are provided with this paper.

References:

1. Goldberg, D. S. & McGee, S. J. Pain as a global public health priority. *BMC Public Health* **11**, 770 (2011).
2. Fine, P. G. Long-term consequences of chronic pain: mounting evidence for pain as a neurological disease and parallels with other chronic disease states. *Pain Medicine* **12**, 996-1004 (2011).
3. Pitcher, M. H., Von Korff, M., Bushnell, M. C & Porter, L. Prevalence and profile of high impact chronic pain in the United States. *Journal of Pain* **20**,146-160 (2019).
4. Okie, S. A flood of opioids, a rising tide of deaths. *N. Engl. J. Med*. **363**, 1981-1985 (2010).
5. Ballantyne, J. C. Opioids for the treatment of chronic pain: mistakes made, lessons learned, and future directions. *Anesth. Analg*. **125**, 1769-1778 (2017).
6. Paulozzi, L. J., Weisler, R. H. & Patkar, A. A. A national epidemic of unintentional prescription opioid overdose deaths: how physicians can help control it. *J. Clin. Psychiatry* **72**, 589-592 (2011).
7. Bronstein, J. M. et al. Deep brain stimulation for Parkinson disease: an expert consensus and review of key issues. *Arch Neurol*. **68**,165 (2011).
8. Boccard S. G., Pereira, E. A. & Aziz, T. Z. Deep brain stimulation for chronic pain. *J. Clin Neurosci*. **22**, 1537-1543 (2015).
9. Johnson, M. D. et al. Neuromodulation for brain disorders: challenges and opportunities. *IEEE Trans. Biomed Eng.* **60**, 610-624 (2013).
10. Wagner, T., Valero-Cabre, A. & Pascual-Leone, A. Noninvasive human brain stimulation. *Annu. Rev. Biomed. Eng.* **9**,527-565 (2007).
11. Mayberg, H. S. et al. Deep brain stimulation for treatment-resistant depression. *Neuron* **45**,651-60 (2005).
12. Bennabi D. & Haffen, E. Transcranial direct current stimulation (tDCS): a promising treatment for major depressive disorder? *Brain Sci.* **8**, 81 (2018).
13. Lefaucheur, J. P., Drouot, X., Keravel, Y. & Nguyen, J. P. Pain relief induced by repetitive transcranial magnetic stimulation of precentral cortex. *Neuroreport*. **12**, 2963-5 (2001).
14. Knotkova, H., Leuschner, Z., Soto, E., Greenberg, A. & Cruciani, R. A. Evaluation of outcomes from transcranial direct current stimulation (tDCS) for the treatment of chronic pain. *J. Pain* **14**, S64 (2013).
15. Tufail, Y., Yoshihiro, A., Pati, S., Tauchmann, M. L. & Tyler, W. J. Ultrasonic neuromodulation by brain stimulation with transcranial ultrasound. *Nat. Protoc*. **6**, 1453-1470 (2011).
16. Yoo, S. S. et al. Focused ultrasound modulates region-specific brain activity. *Neuroimage* **56**, 1267-1275 (2011).
17. Min, B. K. et al. Focused ultrasound modulates the level of cortical neurotransmitters: potential as a new functional brain mapping technique. *International Journal of Imaging Systems and Technology* **21**,232-240 (2011).
18. Fry, F. J., Ades, H. W. & Fry, W. J. Production of reversible changes in the central nervous system by ultrasound. *Science* **127**, 83-4 (1958).
19. Foster, K. R. & Wiederhold, M. L. Auditory responses in cats produced by pulsed ultrasound. *J. Acoust. Soc. Am*. **63**,1199–205 (1978).

20. Martínez-Fernández, R. et al. Focused ultrasound subthalamotomy in patients with asymmetric Parkinson's disease: a pilot study. *Lancet Neurol*. **17**, 54-63 (2018).
21. Fasano, A. et al. Magnetic resonance imaging-guided focused ultrasound thalamotomy in parkinson tremor: reoperation after benefit decay. *Mov Disord*. **33**, 848-9 (2018).
22. Beisteiner, R. et al. Transcranial pulse stimulation with ultrasound in Alzheimer's disease-a new navigated focal brain therapy. *Adv Sci*. **7,** 1902583 (2019).
23. Lipsman, N. et al. Blood–brain barrier opening in Alzheimer's disease using MR-guided focused ultrasound. *Nat. Commun*. **9**, 2336 (2018).
24. Mooney, S. J., Nobrega, J. N., Levitt, A. J. & Hynynen, K. Antidepressant effects of focused ultrasound induced blood-brain-barrier opening. *Behav Brain Res*. **342**, 57-61 (2018).
25. Badran, B. W. et al. Sonication of the anterior thalamus with MRI-guided transcranial focused ultrasound, (tFUS) alters pain thresholds in healthy adults: a double-blind, sham-controlled study. *Brain Stimul*. **13**,1805–12 (2020).
26. Hameroff, S. et al. Transcranial ultrasound (TUS) effects on mental states: a pilot study. *Brain Stimul*. **6**, 409-15 (2013).
27. Zhang, T. et al. Transcranial focused ultrasound stimulation of periaqueductal gray for analgesia. *IEEE Trans Biomed Eng*. 10.1109/TBME.2022.3162073 (2022).
28. Bushnell, M. C., Ceko, M. & Low, L. A. Cognitive and emotional control of pain and its disruption in chronic pain. *Nat Rev Neurosci*. **14**, 502-11 (2013).
29. Peirs, C. & Seal, R. P. Neural circuits for pain: recent advances and current views. *Science* **354**, 578-584 (2016).
30. Mercer, L. N., Chen, C., Gilam, G., Mackey, S. & Scherrer, G. Brain circuits for pain and its treatment. *Sci Transl Med*. **13**, eabj7360 (2021).
31. Mogil, J. S. Animal models of pain: progress and challenges. *Nat. Rev. Neurosci*. **4**, 283-94 (2009).
32. Deuis, J. R., Dvorakova, L. S. & Vetter, I. Methods used to evaluate pain behaviors in rodents. *Front Mol Neurosci*. **10**, 284 (2017).
33. Cain, D. M., Vang, D., Simone, D. A., Hebbel, R. P. & Gupta, K. Mouse models for studying pain in sickle disease: effects of strain, age, and acuteness. *Br J Haematol*. **156**, 535-544 (2011).
34. Tran, H., Gupta, M. & Gupta, K. Targeting novel mechanisms of pain in sickle cell disease. *Blood* **130**, 2377-2385 (2017).
35. Kohli, D. R. et al. Pain-related behaviors and neurochemical alterations in mice expressing sickle hemoglobin: modulation by cannabinoids. *Blood* **116**, 456-65 (2010).
36. Hillery, C. A. et al. Transient receptor potential vanilloid 1 mediates pain in mice with severe sickle cell disease. *Blood* **118**, 3376-83 (2011).
37. Brandow, A. M., Weisman, S. J. & Panepinto, J. A. The impact of a multidisciplinary pain management model on sickle cell disease pain hospitalizations. *Pediatr Blood Cancer* **56**, 789-93 (2011).
38. Smith, W. R. et al. Daily assessment of pain in adults with sickle cell disease. *Ann Intern Med*. **148**, 94-101 (2008).
39. Lei, J., Benson, B., Tran, H., Ofori-Acquah, S. F. & Gupta, K. Comparative analysis of pain behaviours in humanized mouse models of sickle cell anemia. *PLoS One* **11**, e0160608 (2016).

40. Petrus, M. et al. A role of TRPA1 in mechanical hyperalgesia is revealed by pharmacological inhibition. *Mol. Pain*. **3**, 40 (2007).
41. Gritsch, S., Bali, K. K., Kuner, R. & Vardeh, D. Functional characterization of a mouse model for central post-stroke pain. *Mol Pain*. **12**, 1744806916629049 (2016).
42. Deuis, J. R. et al. An animal model of oxaliplatin-induced cold allodynia reveals a crucial role for Nav1.6 in peripheral pain pathways. *Pain* **154**, 1749-1757 (2013).
43. Allchorne, A. J., Broom, D. C. & Woolf, C. J. Detection of cold pain, cold allodynia and cold hyperalgesia in freely behaving rats. *Mol. Pain* **1**, 36 (2005).
44. Yu, K., Niu, X., Krook-Magnuson, E & He, B. Intrinsic functional neuron-type selectivity of transcranial focused ultrasound neuromodulation. *Nat Commun* **12**, 2519 (2021)
45. Lavich, T. R., Cordeiro, R. S., Silva, P. M. & Martins, M. A. A novel hot-plate test sensitive to hyperalgesic stimuli and non-opioid analgesics. *Braz J Med Biol Res*. **38**, 445-451 (2005).
46. Bartley, E. J. & Fillingim, R. B. Sex differences in pain: a brief review of clinical and experimental findings. *Br J Anaesth*. **111**, 52-8 (2013).
47. Mogil, J. S. Sex differences in pain and pain inhibition: multiple explanations of a controversial phenomenon. *Nat Rev Neurosci*. **13**, 859-66 (2012).
48. Staikou, C. et al. Differences in pain perception between men and women of reproductive age: a laser-evoked potentials study. *Pain Med*. **18**, 316-321 (2017).
49. Feng, X. et al. Transcranial ultrasound stimulation of the anterior cingulate cortex reduces neuropathic pain in mice. *Evid Based Complement Alternat Med*. **2021**, 6510383 (2021).
50. Kim, H., Park, M. Y., Lee, S. D., Lee, W., Chiu, A. & Yoo, S. S. Suppression of EEG visual-evoked potentials in rats through neuromodulatory focused ultrasound. *Neuroreport*. **26**, 211-5 (2015).
51. Plaksin, M., Kimmel, E. & Shoham, S. Cell-type-selective effects of intramembrane cavitation as a unifying theoretical framework for ultrasonic neuromodulation. *eNeuro*. **3**, 0136-15 (2016).
52. Deacon, R. M. Measuring motor coordination in mice. *J Vis Exp*. **75**, e2609 (2013).
53. Jakkamsetti, V. et al. Quantification of early learning and movement sub-structure predictive of motor performance. *Sci Rep* **11**, 14405 (2021).
54. Gaur, P. et al. Histologic safety of transcranial focused ultrasound neuromodulation and magnetic resonance acoustic radiation force imaging in rhesus macaques and sheep. *Brain Stimul*. **13**, 804-814 (2020).
55. Lei, J. et al. Heme causes pain in sickle mice via toll-like receptor 4-mediated reactive oxygen species- and endoplasmic reticulum stress-induced glial activation. *Antioxid Redox Signal* **34**, 279-293 (2021).
56. Iaccarino, H. et al. Gamma frequency entrainment attenuates amyloid load and modifies microglia. *Nature* **540**, 230-235 (2016).
57. Martorell, A. J. et al. Multi-sensory gamma stimulation ameliorates alzheimer's-associated pathology and improves cognition. *Cell* **177**, 256-271 (2019).
58. Tan, L. L. et al. Gamma oscillations in somatosensory cortex recruit prefrontal and descending serotonergic pathways in aversion and nociception. *Nat Commun*. **10**, 983 (2019).

59. Naghdi, L., Ahonen, H., Macario, P. & Bartel, L. The effect of low-frequency sound stimulation on patients with fibromyalgia: a clinical study. *Pain Res Manag*. **20**, e21-7 (2015).
60. Kantor, J. et al. Exploring vibroacoustic therapy in adults experiencing pain: a scoping review. *BMJ Open* **12**, e046591 (2022).
61. He, Y. et al. CaMKIIα underlies spontaneous and evoked pain behaviors in Berkeley sickle cell transgenic mice. *Pain* **157**, 2798-2806 (2016).
62. Cataldo, G., Rajput, S., Gupta, K. & Simone, D. A. Sensitization of nociceptive spinal neurons contributes to pain in a transgenic model of sickle cell disease. *Pain* **156**, 722-730 (2015).
63. Hunskaar, S., Berge, O. G. & Hole, K. A modified hot-plate test sensitive to mild analgesics. *Behav Brain Res*. **21**, 101-8 (1986).
64. Plone, M. A., Emerich, D. F. & Lindner, M. D. Individual differences in the hotplate test and effects of habituation on sensitivity to morphine. *Pain* **66**, 265-70 (1996).
65. Lane, D. A. & Morgan, M. M. Antinociceptive tolerance to morphine from repeated nociceptive testing in the rat. *Brain Res*. **1047**, 65-71 (2005).
66. Gunn, A., Bobeck, E. N., Weber, C. & Morgan, M. M. The influence of non-nociceptive factors on hot-plate latency in rats. *J Pain* **12**, 222-7 (2011).
67. Lee, W. How to interpret the ultrasound output display standard for higher acoustic output diagnostic ultrasound devices. *J Ultrasound Med*. **17**, 535-8 (1998).
68. Nelson, T. R., Fowlkes, J. B., Abramowicz, J. S. & Church, C. C. Ultrasound biosafety considerations for the practicing sonographer and sinologist. *J Ultrasound Med.* **28**, 139-150 (2009).
69. Tufail, Y. et al. Transcranial Pulsed Ultrasound Stimulates Intact Brain Circuits. *Neuron* **66**, 681-694 (2010).
70. Fisher, J. A. N. & Gumenchuk, I. Low-intensity focused ultrasound alters the latency and spatial patterns of sensory-evoked cortical responses in vivo. *Journal of Neural Engineering* **15**, 035004 (2018).
71. Kim, H., Chiu, A., Lee, S. D., Fischer, K. & Yoo, S. S. Focused ultrasound-mediated non-invasive brain stimulation: examination of sonication parameters. *Brain Stimul* **7**, 748-756 (2014).
72. Kim, H. et al. Noninvasive transcranial stimulation of rat abducens nerve by focused ultrasound. *Ultrasound in medicine & biology* **38**, 1568-1575 (2012).
73. Yoo, S. S. et al. Focused ultrasound modulates region-specific brain activity. *NeuroImage* **56**, 1267-1275 (2011).
74. Kim, H. et al. Transcranial focused ultrasound modulates cortical and thalamic motor activity in awake sheep. *Scientific Reports* **11**, 19274 (2021).
75. Verhagen, L. et al. Offline impact of transcranial focused ultrasound on cortical activation in primates. *Elife* **8**, e40541 (2019).
76. Lin, Z. et al. Non-invasive ultrasonic neuromodulation of neuronal excitability for treatment of epilepsy. *Theranostics* **10**, 5514-5526 (2020).
77. Manci, E. A. Pathology of berkeley sickle cell mice: similarities and differences with human sickle cell disease. *Blood* **107**, 1651-1658 (2006).
78. Kiven, S. et al. Spatiotemporal alterations in gait in humanized transgenic sickle mice. *Front Immunol*. **11**, 561947 (2020).

79. Wang, L. et al. Cognitive and behavior deficits in sickle cell mice are associated with profound neuropathologic changes in hippocampus and cerebellum. *Neurobiol Dis*. **85**, 60-72 (2016).
80. Barcelon, E. E., Cho, W. H., Jun, S. B. & Lee, S. J. Brain microglial activation in chronic pain-associated affective disorder. *Front Neurosci*. **13**, 213 (2019).
81. Wozniak, K. M., Rojas, C., Wu, Y. & Slusher, B. S. The role of glutamate signaling in pain processes and its regulation by GCP II inhibition. *Curr Med Chem*. **19**, 1323-34 (2012).
82. Enna, S. J. & McCarson, K. E. The role of GABA in the mediation and perception of pain. *Adv Pharmacol*. **54**, 1-27 (2006).
83. Wood, P. B. Role of central dopamine in pain and analgesia. *Expert Rev Neurother*. **8**, 781-97 (2008).
84. Tran, H. et al. Diet and companionship modulate pain via a serotonergic mechanism. *Sci Rep*. **11**, 2330 (2021)
85. Valverde, Y., Benson, B., Gupta, M. & Gupta, K. Spinal glial activation and oxidative stress are alleviated by treatment with curcumin or coenzyme Q in sickle mice. *Haematologica* **101**, e44-7 (2016).
86. King, R. L., Brown, J. R., Newsome, W. T. & Pauly, K. B. Effective parameters for ultrasound-induced in vivo neurostimulation. *Ultrasound Med Biol*. **39**, 312-31 (2013).
87. King, R. L., Brown, J. R. & Pauly, K. B. Localization of ultrasound-induced in vivo neurostimulation in the mouse model. *Ultrasound Med Biol*. **40**, 1512-22 (2014).
88. Li, G. F. et al. Improved anatomical specificity of non-invasive neuro-stimulation by high frequency (5 MHz) ultrasound. *Sci Rep* **6**, 24738 (2016).
89. Sunkin, S. M. et al. Allen Brain Atlas: An integrated spatio-temporal portal for exploring the central nervous system. *Nucleic Acids Res*. **41**, D996–D1008 (2013).
90. Allen Institute for Brain Science. Allen Mouse Common Coordinate Framework. http://help.brain-map.org/display/mouseconnectivity/Documentation (2017).
91. Oh, S. W. et al. A mesoscale connectome of the mouse brain. *Nature* **508**, 207-214 (2014).
92. Sagi, V., Song-Naba, W. L., Benson, B. A., Joshi, S. S. & Gupta, K. Mouse models of pain in sickle cell disease. *Curr Protoc Neurosci*. **85**, e54 (2018).
93. Pászty, C. et al. Transgenic knockout mice with exclusively human sickle hemoglobin and sickle cell disease. *Science* **278**, 876-8 (1997).
94. Tang, S. C. & Clement, G. T. Standing-wave suppression for transcranial ultrasound by random modulation. *IEEE transactions on Biomedical Engineering* **57**, 203-205 (2009).
95. Blackstock, D. T. Fundamentals of Physical Acoustics. John Wiley&Sons, Inc., New York (2000).
96. Bonin, R. P., Bories, C. & De Koninck, Y. A simplified up-down method (SUDO) for measuring mechanical nociception in rodents using von Frey filaments. *Mol Pain* **10**, 26 (2014).
97. Kohli, D. R. et al. Pain-related behaviors and neurochemical alterations in mice expressing sickle hemoglobin: modulation by cannabinoids. *Blood* **116**, 456–65 (2010).

98. Vincent, L. et al. Cannabinoid receptor-specific mechanisms to alleviate pain in sickle cell anemia via inhibition of mast cell activation and neurogenic inflammation. *Haematology* **101**, 566–577 (2015).

Tables and Figures

Table 1: Registered coordinates of ultrasound focus on respective brain targets based on Allen Mouse Brain Atlas[89,90,91]

Target*	Sham (mm)	Left S1HL (mm)	Left thalamus (mm)	Left insula (mm)
X	0	1.77	1.27	3.17
Y	-3.50	-4.73	-5.77	-3.05
Z	-0.08	-0.08	2.70	3.36

*Note: All registered coordinates are relative to the reference location depicted in Fig. 1b.

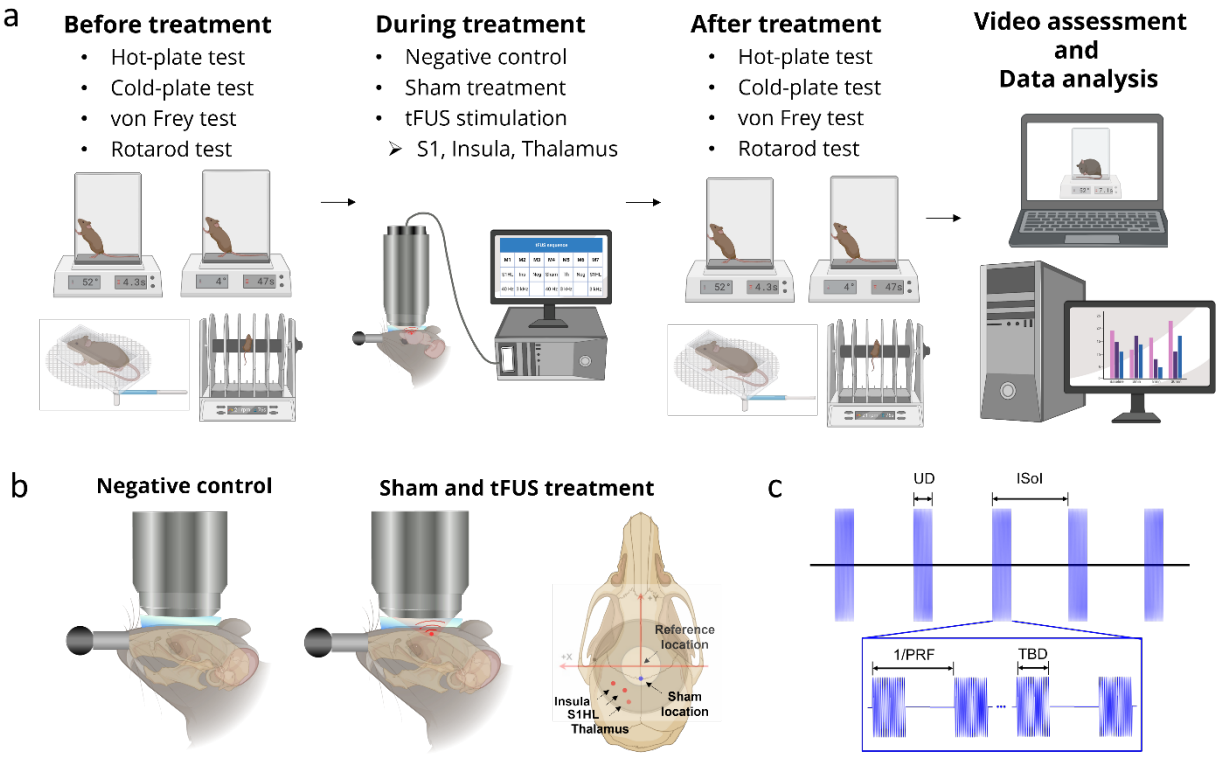

Fig. 1 | Experimental configuration of behavioral study and tFUS stimulation with multiple controls. a, Schematic of experimental setup consisted of various behavioral test, tFUS stimulation with several control groups, and video evaluation with data analysis. To investigate the effect of tFUS stimulation to the various brain locations such as S1, insula, and thalamus, behavioral nocifensive reactions to heat, cold, and mechanical stimuli and motor performance were recorded and assessed. **b,** To determine whether the modulatory effect is specific to tFUS stimulation at a specific brain circuit, the effects of negative control (i.e., not applying tFUS stimulation, but maintaining all experimental procedures) and sham treatment (i.e., applying tFUS to a control brain structure near the targeted brain location) were examined. **c,** The customized 128-element random array transducer is to steer ultrasound focus. Each brain structure was targeted by tFUS at a center frequency of 1.5 MHz, tone-burst duration (TBD) of 200 μs, pulse repetition frequency (PRF) of 40 Hz and 3 kHz, ultrasound duration (UD) of 400 ms, inter-sonication interval (ISoI) of 4 s, and total sonication time of 10 min, 20 min, and 1 h.

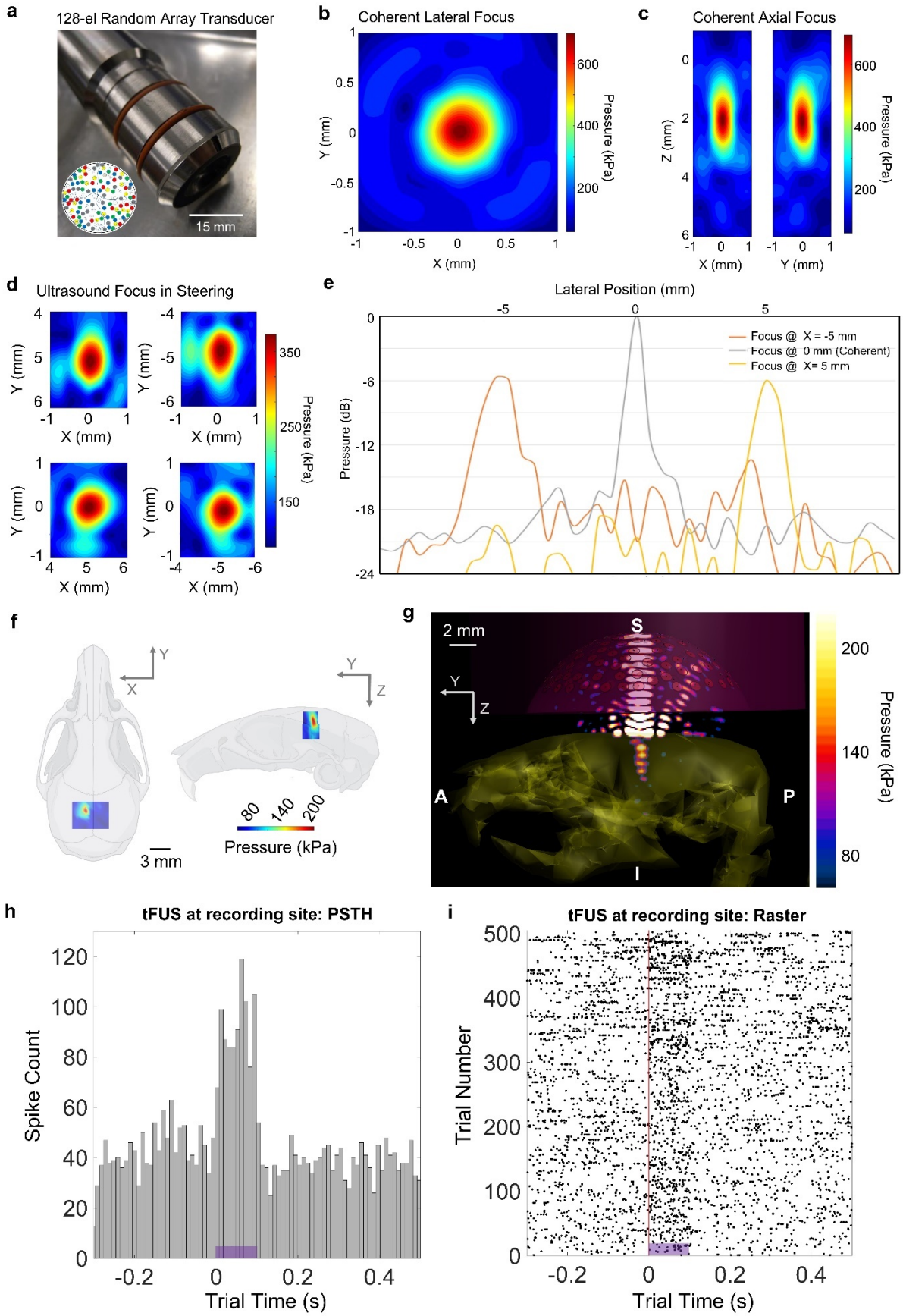
a
128-el Random Array Transducer
15 mm
b
Coherent Lateral Focus
Y (mm)
X (mm)
Pressure (kPa)
c
Coherent Axial Focus
Z (mm)
X (mm)
Y (mm)
Pressure (kPa)
d
Ultrasound Focus in Steering
Y (mm)
X (mm)
Pressure (kPa)
e
Lateral Position (mm)
Pressure (dB)
Focus @ X = -5 mm
Focus @ 0 mm (Coherent)
Focus @ X= 5 mm
f
Y
X
Z
3 mm
Pressure (kPa)
g
2 mm
S
A
P
I
Pressure (kPa)
h
tFUS at recording site: PSTH
Spike Count
Trial Time (s)
i
tFUS at recording site: Raster
Trial Number
Trial Time (s)

Fig. 2 | Characterizations of ultrasound field generated by the ultrasound neuromodulation probe and validations of its *in vivo* targeting. a, The device photo of 128-element random array ultrasound transducer (H276). The inset shows the element layout across the acoustic aperture. **b-c,** Physically measured coherent lateral (panel **b**) and axial (panel **c**) focal performances of H276 in free water when the probe was powered by the Vantage 128 system. **d,** Characterizations of steered ultrasound focus at X = ±5 mm and Y = ±5 mm. **e,** The line profiles of the generated ultrasound pressures when the ultrasound focus was located at X = 0 mm, -5 mm or 5 mm. **f,** The transcranial ultrasound field physically measured with hydrophone in the presence of a mouse skull top in horizontal (left) and sagittal (right) views. **g,** The simulated ultrasound pressure field generated by H276 (all 128 elements transmitted coherently) within an intact adult mouse skull cavity. **h-i,** Time-locked increase of neuronal spiking activities elicited by tFUS when stimulating at a hindlimb representation area of somatosensory cortex (S1HL), where an intracranial recording electrode was placed. The peri-stimulus time histogram (PSTH, time bin size: 10 ms) and the raster plot exhibited tFUS-induced neuronal activations, and the sonication duration is demonstrated with purple bars.

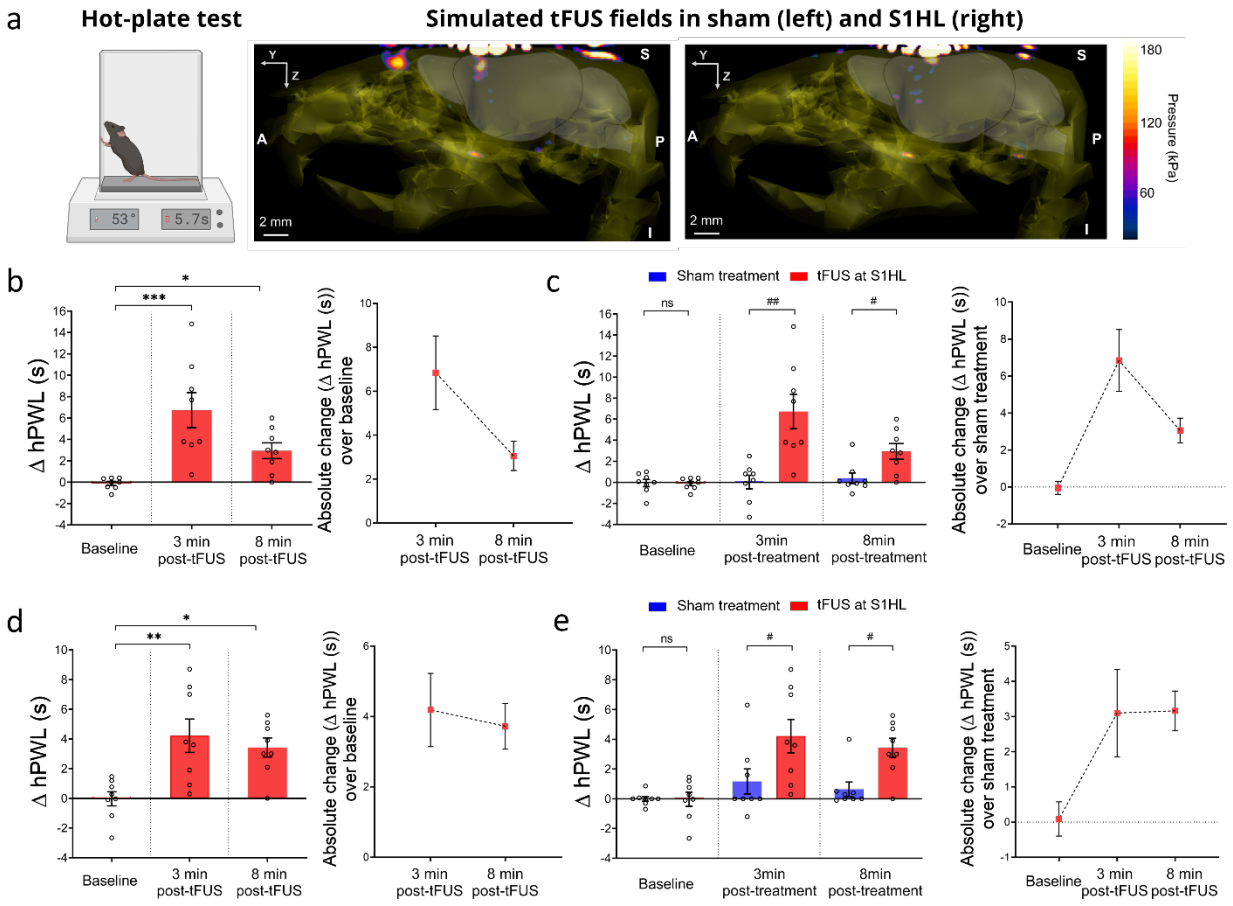

Fig. 3 | Short-term reduction of heat pain-related behaviors by the single-session tFUS stimulation in wild-type mice. a, Behavioral nocifensive reaction to noxious heat with pre-determined temperature of 53°C was blindly examined. Left cortical hemisphere of S1HL and sham location at the midline (ΔX = -1.77 mm, ΔY = 1.225 mm, relative to the targeting region at the S1HL were stimulated. The simulated tFUS fields with the mouse skull cavity was co-registered with a mouse brain atlas in sham location and S1HL. The unilateral effect of the tFUS stimulation with PRF of 40 Hz and sham treatment was investigated by comparing the latency of the ipsilateral and contralateral hind paw withdrawal responses. **b,c,** A significant increase in the latency differences between ipsilateral and contralateral hind paw withdrawal (Δ hind paw withdrawal latency (hPWL) = contralateral (right) hPWL - ipsilateral (left) hPWL) was observed in male wild-type mice compared to the pre-stimulation baseline (left) and latency time from sham-treated mice (right) (animal number N=8 for single-session tFUS with a PRF of 40 Hz and sham treatment). **d-e,** tFUS-induced remarkable change of Δ hPWL was observed in female wild-type mice against the baseline (left) as well as the response from sham treatment (right) (N=8 for tFUS and sham stimulation). Statistical analysis was conducted with one-way ANOVA with Friedman test, *p<0.05, **p<0.01, ***p<0.001; t-test with Mann-Whitney test, ns: not significant, #p<0.05, ##p<0.01. Data are shown as mean ± standard error of the mean (s.e.m.).

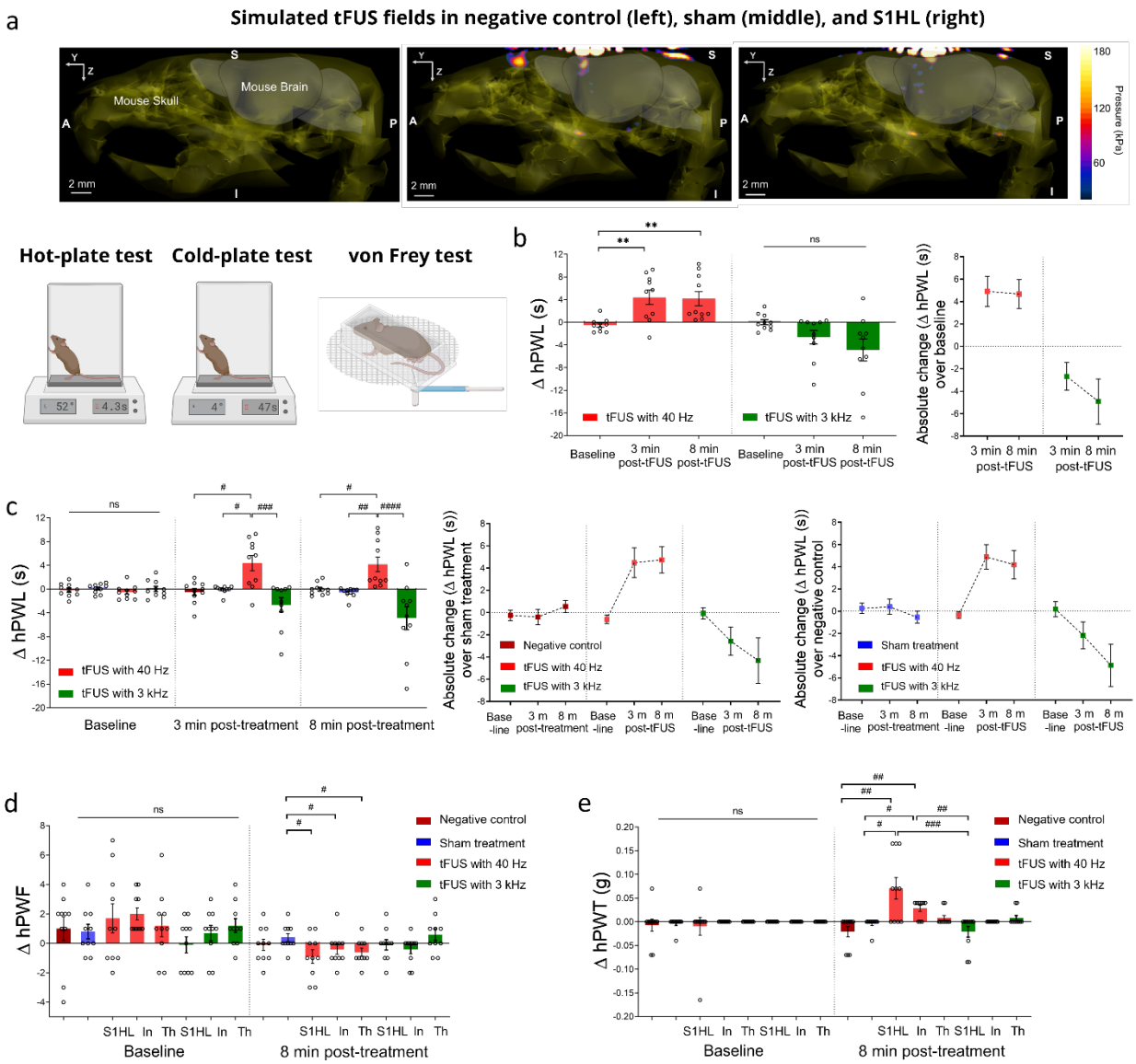

Fig. 4 | Short-term modulation of thermal (heat and cold) and mechanical hyperalgesia with the single-session tFUS stimulation in HbSS-BERK mice. a, The simulated tFUS fields with the mouse skull cavity was conducted and co-registered with a mouse brain atlas in negative control, sham location, and S1HL. The quantification of averaged Δ hPWL from hot-plate test, Δ hind paw withdrawal frequency (Δ hPWF) from cold-plate test, and Δ hind paw withdrawal threshold (Δ hPWT) from von Frey test was conducted before and after targeting S1HL, insula, and thalamus with controls (negative control and sham treatment) in HbSS-BERK mice. **b-c,** The single-session tFUS with a PRF of 40 Hz at left S1HL led to a significant increase in the averaged Δ hPWL in HbSS-BERK mice compared to the baseline value (**b,** N=10 for tFUS stimulation with a PRF of 40 Hz) as well as sham treatment and negative control (**c,** N=10 for sham stimulation and negative control), whereas the control groups did not show apparent treatment effect compared to pre-treatment baseline. In addition, a negative value of Δ hPWL was observed by the single-session tFUS stimulation with a PRF of 3 kHz at left S1HL, which

was significantly different from the response with tFUS with the PRF of 40 Hz (**c,** left, N=10 for tFUS stimulation with the PRF of 3 kHz and 40 Hz). **D,** Compared to the sham treatment, the single-session tFUS with the PRF of 40 Hz at S1HL, insula, and thalamus led to a significant change in the Δ hPWF at 8 min after treatment (N=10 for sham stimulation and tFUS stimulation with the PRF of 40 Hz at S1HL, insula, and thalamus). Note that In and Th represent insula and thalamus, respectively. **e,** tFUS with PRF of 40 Hz at left S1HL and insula, but not thalamus region, resulted in a prominent elevation of Δ hPWT compared to the sham-treated and negative control mice (N=10 for sham treatment and negative control). In addition, a lower threshold of the withdrawal response of the contralateral (right) hind paw was observed by tFUS with the PRF of 3 kHz at left S1HL as compared to the threshold from ipsilateral (left) hind paw (**e,** N=10 for tFUS stimulation with the PRF of 3 kHz at S1HL, insula, and thalamus). Statistical analysis was conducted with one-way ANOVA with Friedman test and t-test with Wilcoxon matched-pairs signed rank test, ns: not significant, $^{**}p<0.01$; one-way ANOVA with Kruskal-Wallis test and t-test with Mann-Whitney test, $^{\#}p<0.05$, $^{\#\#}p<0.01$, $^{\#\#\#}p<0.001$, $^{\#\#\#\#}p<0.0001$. Data are shown as mean ± s.e.m.

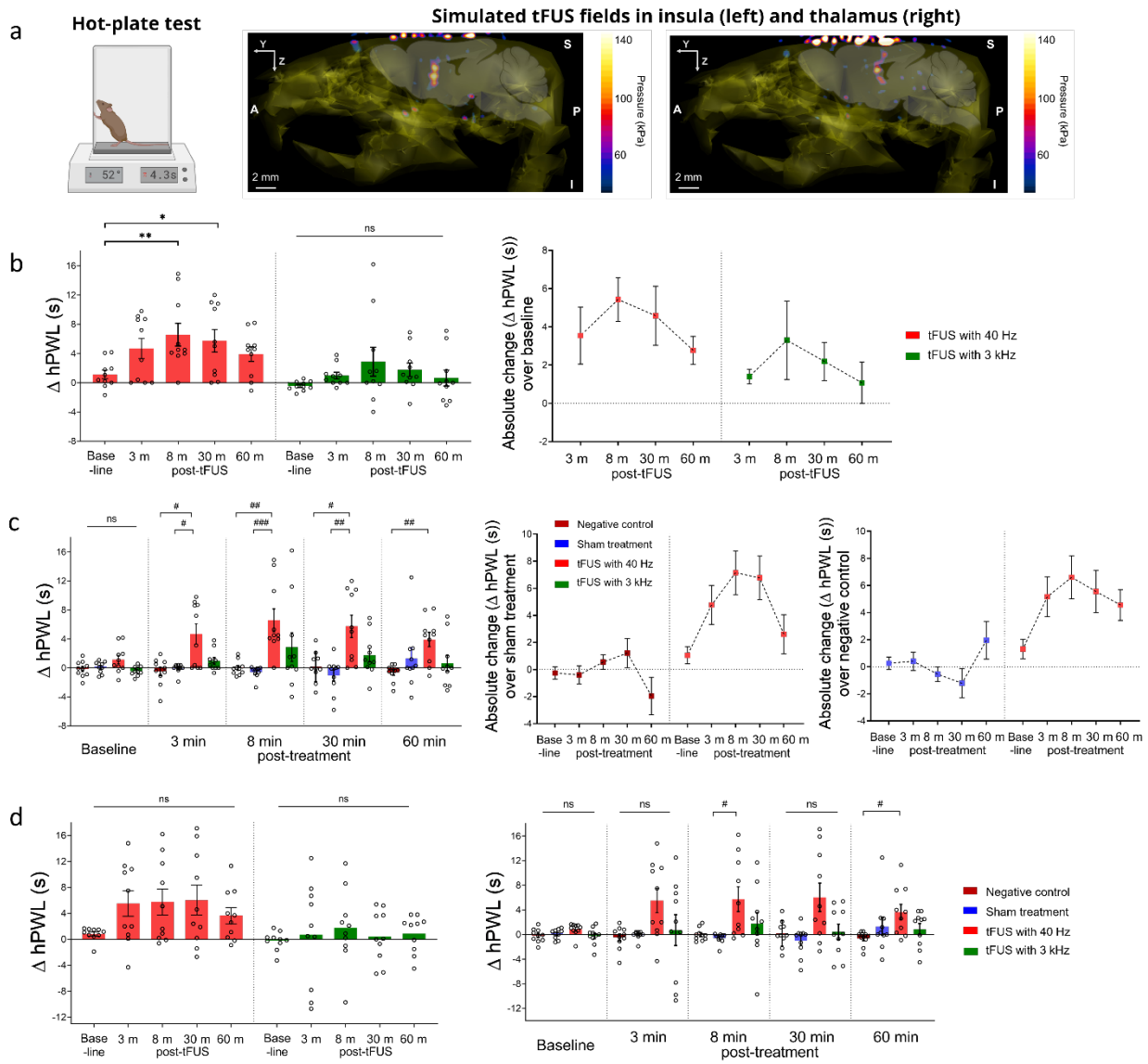

Fig. 5 | Sustained modulatory effect of heat hyperalgesia with the single-session tFUS stimulation in female HbSS-BERK mice. a, The simulated tFUS fields within the mouse skull cavity was co-registered with a mouse brain atlas in the insula and thalamus. Sustained effect of tFUS stimulation on the behavioral response to noxious heat was investigated by stimulating the deep cortical structure, i.e., insula and the deep brain target, i.e., thalamus. **b-c,** The averaged Δ hPWL stimulated by single-session tFUS with a PRF of 40 Hz at left insula was significantly increased up to 30 min in HbSS-BERK mice compared to the pre-tFUS baseline (**b,** N=10 for tFUS stimulation with PRF of 40 Hz) as well as value from sham and negative control groups (**c,** N=10 for sham treatment and negative control). However, the single-session tFUS with a PRF of 3 kHz, sham treatment, and negative control did not lead to remarkable changes in Δ hPWL compared to the baseline (N=10 for tFUS with the PRF of 3 kHz). **d,** Targeting thalamus with tFUS with the PRF of 40 Hz and 3 kHz did not result in a prominent modulatory effect compared to the pre-stimulation baseline (left, N=10 for tFUS stimulation with the PRF of 40 Hz and 3

kHz) as well as sham-treated mice and negative control mice (right, N=10 for sham treatment and negative control). Statistical analysis was conducted with one-way ANOVA with Friedman test, ns: not significant, *$p<0.05$, **$p<0.01$; one-way ANOVA with Kruskal-Wallis test, $^{\#}p<0.05$, $^{\#\#}p<0.01$, $^{\#\#\#}p<0.001$. Data are shown as mean ± s.e.m.

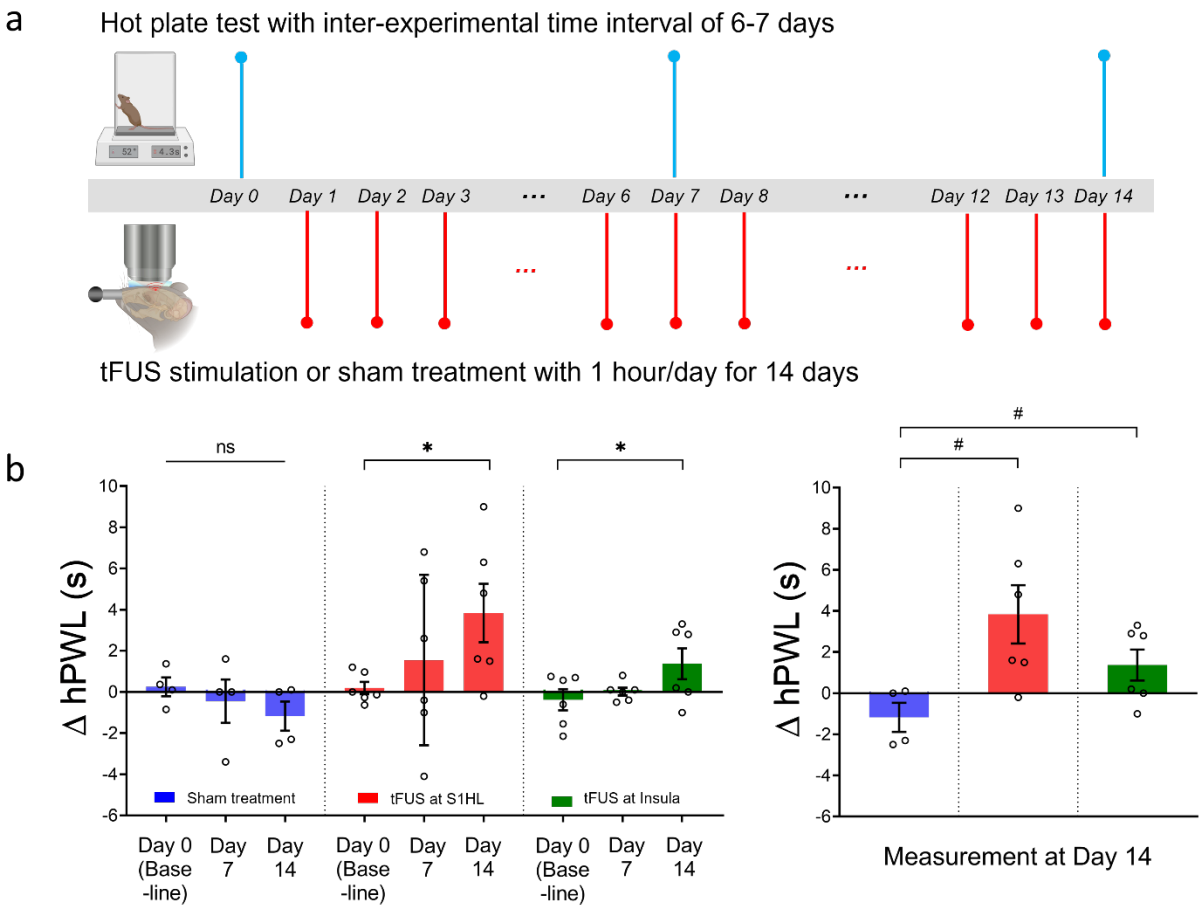

Fig. 6 | Long-lasting modulatory effect of heat hyperalgesia with multi-session tFUS stimulation in aged female HbSS-BERK mice. a, Long-term suppression of heat hyperalgesia was investigated in aged female HbSS-BERK mice ranging from 11 to 15 month-old by measuring latency from noxious heat stimuli at every 6-7 days from pre-stimulation baseline. The behavioral reaction to the heat stimulus along with a repeated tFUS stimulation for 14 days with 1 h per day was assessed and compared with the baseline and sham-treated behavioral response to heat stimuli. **b-c,** After multi-session tFUS stimulation with a PRF of 40 Hz to S1HL or insula for 14 days, the averaged changes of Δ hPWL were significantly increased compared to the baseline values (**b,** N=6 for tFUS to S1HL and insula) as well as sham-treated behavioral change (**c,** N=4 for sham treatment). Given the measurement time at 2 h after tFUS or sham treatment, the effect of multi-session tFUS stimulation is maintained for at least 2 h. Statistical analysis was conducted with t-test with Wilcoxon one-tailed signed rank test, ns: not significant, $^{*}p<0.05$; t-test with one-tailed Mann-Whitney test, $^{\#}p<0.05$. Data are shown as mean ± s.e.m.

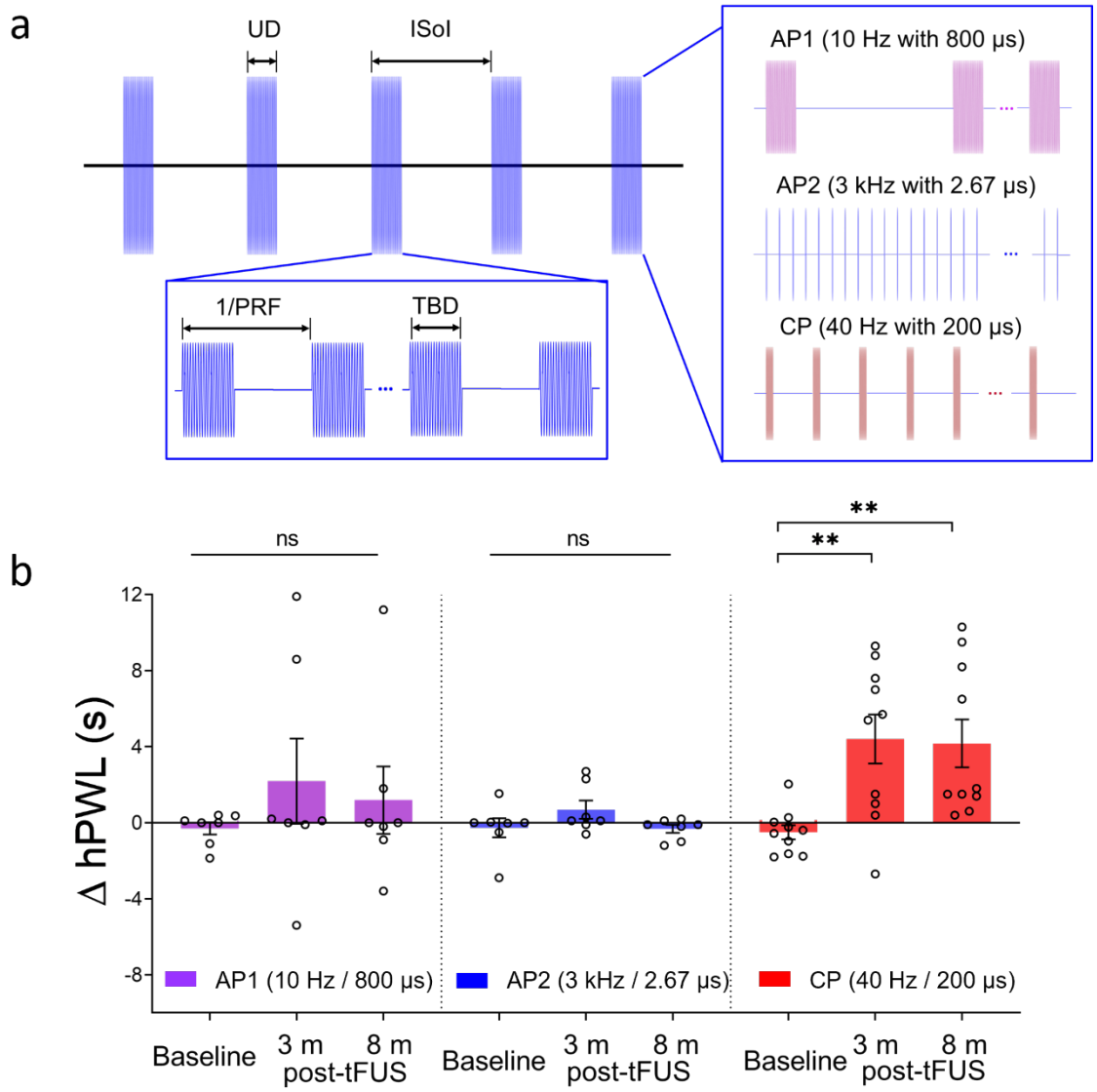

Fig. 7 | Ultrasound parameter study. a, The effect of different PRF values (maintaining the same ultrasound burst duty cycle and transmitted energy) on heat pain-associated behavior was investigated. Given the same duty cycle of 0.8%, additional parameter1 (AP1) with PRF of 10 Hz and TBD of 800 μs) and AP2 with PRF of 3 kHz and TBD of 2.67 μs were selected and applied at S1HL without changing the rest of the tFUS experimental setup, which was further compared with the current parameter (CP) of PRF of 40 Hz and TBD of 200 μs. **b,** The single-session tFUS with AP1 and AP2 did not induce a marked change in behavioral response to heat stimuli in HbSS-BERK mice compared to pre-stimulation baseline (N=7 for tFUS with AP1 and AP2; N=10 for tFUS with CP). Statistical analysis was conducted with one-way ANOVA with Friedman test, ns: not significant, ***p*<0.01. Data are shown as mean ± s.e.m.

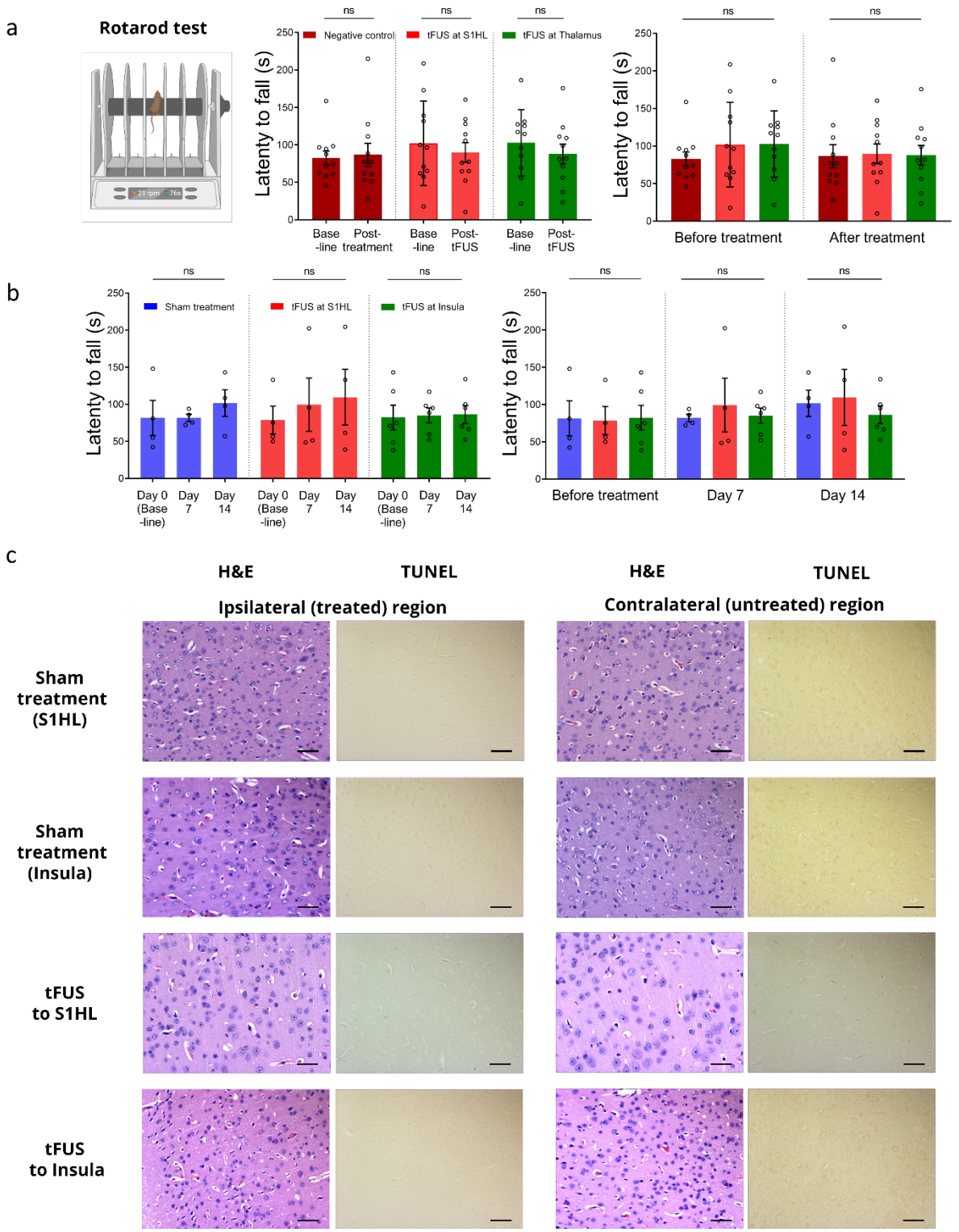

Fig. 8 | tFUS safety evaluation in female HbSS-BERK mice. a-b, The effect of tFUS on the motor coordination and balance was investigated in rotarod testing (left). After single-session tFUS stimulation with a PRF of 40 Hz to S1HL or thalamus and multi-session tFUS with the PRF of 40 Hz to S1HL or insula for 14 days with 1 h per day, we

did not find any significant alteration in the averaged latency to fall compared with pre-stimulation baseline (**a,** middle, N=11 for single-session tFUS stimulation with the PRF of 40 Hz at S1HL and thalamus; **b,** left, N=4 and 6 for multi-session tFUS with the PRF of 40 Hz at S1HL and insula, respectively). Statistical analysis was conducted with t-test with Wilcoxon matched-pairs signed rank test and one-way ANOVA with Kruskal-Wallis test, ns: not significant. Data are shown as mean ± s.e.m. **c,** Double-blind histological analysis using H&E and TUNEL stains showed that multi-session tFUS stimulation to left S1HL or insula had no adverse impact on the tissue structural integrity and nuclear morphology within treated brain region when comparing with contralateral brain regions and sham treatment in HbSS-BERK mice. The scale bars for both H&E and TUNEL images are 50 μm.